Rail. Eng. Science (2022) 30(4):437–467
https://doi.org/10.1007/s40534-022-00281-2

Pantograph–catenary electrical contact system of high-speed railways: recent progress, challenges, and outlooks

Guangning Wu[1] · Keliang Dong[1] · Zhilei Xu[1] · Song Xiao[1] · Wenfu Wei[1] · Huan Chen[1] · Jie Li[1] · Zhanglin Huang[1] · Jingwei Li[2] · Guoqiang Gao[1] · Guozheng Kang[2] · Chuanjun Tu[3] · Xingyi Huang[4]

Received: 2 November 2021 / Revised: 7 June 2022 / Accepted: 10 June 2022 / Published online: 2 August 2022

Abstract As the unique power entrance, the pantograph–catenary electrical contact system maintains the efficiency and reliability of power transmission for the high-speed train. Along with the fast development of high-speed railways all over the world, some commercialized lines are built for covering the remote places under harsh environment, especially in China; these environmental elements including wind, sand, rain, thunder, ice and snow need to be considered during the design of the pantograph–catenary system. The pantograph–catenary system includes the pantograph, the contact wire and the interface—pantograph slide. As the key component, this pantograph slide plays a critical role in reliable power transmission under dynamic condition. The fundamental material characteristics of the pantograph slide and contact wire such as electrical conductivity, impact resistance, wear resistance, etc., directly determine the sliding electrical contact performance of the pantograph–catenary system; meanwhile, different detection methods of the pantograph–catenary system are crucial for the reliability of service and maintenance. In addition, the challenges brought from extreme operational conditions are discussed, taking the Sichuan–Tibet Railway currently under construction as a special example with the high-altitude climate. The outlook for developing the ultra-high-speed train equipped with the novel pantograph–catenary system which can address the harsher operational environment is also involved. This paper has provided a comprehensive review of the high-speed railway pantograph–catenary systems, including its progress, challenges, outlooks in the history and future.

Keywords High-speed railway · Pantograph–catenary system · Contact wire · Pantograph slide · Status detection

✉ Wenfu Wei
wfwei@home.swjtu.edu.cn

[1] School of Electrical Engineering, Southwest Jiaotong University, Chengdu 610031, China

[2] School of Mechanics and Aerospace Engineering, Southwest Jiaotong University, Chengdu 610031, China

[3] School of Materials Science and Engineering, Hunan University, Changsha 410082, China

[4] Shanghai Key Laboratory of Electrical Insulation and Thermal Ageing, Shanghai Jiaotong University, Shanghai 200240, China

1 Introduction

As a significant strategic support for economic development, high-speed railways bring immense changes in transportation mode of humans all over the world. Compared with the other currently existing transportation tools, the high-speed railway has the outstanding advantages such as high-speed, heavy-load, and being punctual, comfortable, environment-friendly and safe, and therefore has become one of the actively developed infrastructures in the world. In 1964, the world's first high-speed railway was built in Japan with the design speed of 210 km/h. Since then, if the design velocity of a railway is higher than 200 km/h, this line can be defined as a high-speed railway. After that, many countries such as France, Germany and China started to build high-speed railways. The construction and development of high-speed railways in different countries are shown in Table 1. The rapid improvement of high-speed railway running speed leads the development of high-speed trains. For example, the trains with the maximum design speed within the range between 200 and 250 km/h, such as CRH1A and CRH2A, normally can provide a traction power about 5 MW. The trains with the maximum design speed within the range between 250 and 350 km/h, such as CRH2C and CRH3C, normally can

Table 1 High-speed railways of different countries

Countries	Building time (year)	Railway lines	Initial operating speed ($km \cdot h^{-1}$)	Maximum operating speed ($km \cdot h^{-1}$)	National total mileage of operation by 2020 (km)
Japan	1964	Tokaido Shinkansen	210	320	3041
France	1981	Paris–Lyon railway line	270	320	2734
Germany	1991	Mannheim–Stuttgart railway line	250	310	1571
Britain	2003	High Speed 1	225	300	113
China	2007	Suining–Chongqing railway line	200	350	37,900

provide a traction power more than 8.5 MW. The trains with the maximum design speed above 350 km/h, such as CRH380 and CR400, normally can provide a traction power about 10 MW. So far, the highest commercial travel speed of China's high-speed railway has reached 350 km/h, ranking the first in the world. High-speed trains run at high speeds because they are powered by a constant supply of electrical energy, and the entrance to provide electrical energy for the trains is the pantograph–catenary system.

As one of the three basic relationships of high-speed railway (i.e., pantograph–catenary relationship, wheel–rail relationship and fluid–solid relationship), pantograph–catenary system is the key to maintain the constant and reliable power supply for high-speed trains, as shown in Fig. 1a and b, which contains two main components—the catenary and the pantograph [1, 2]. The catenary is a special power supply line built along the track to provide electrical energy for high-speed trains, as it is mainly composed of contact wires. The pantograph is the electrical equipment for high-speed trains to obtain electrical energy from catenary, which is installed on the roof of the train. The interface that directly contacts with the contact wire is pantograph slide. As the key current collection component of the train, the pantograph slide is installed on the top of the pantograph. The pantograph–catenary system provides electric energy for trains through sliding electric contact, which is the only path of energy supply for high-speed trains.

The ideal electrical contact condition between pantograph and catenary is the guarantee of safe and stable current collection of trains. The current collection quality of the pantograph–catenary electrical contact system directly determines whether the train is able to operate safely and

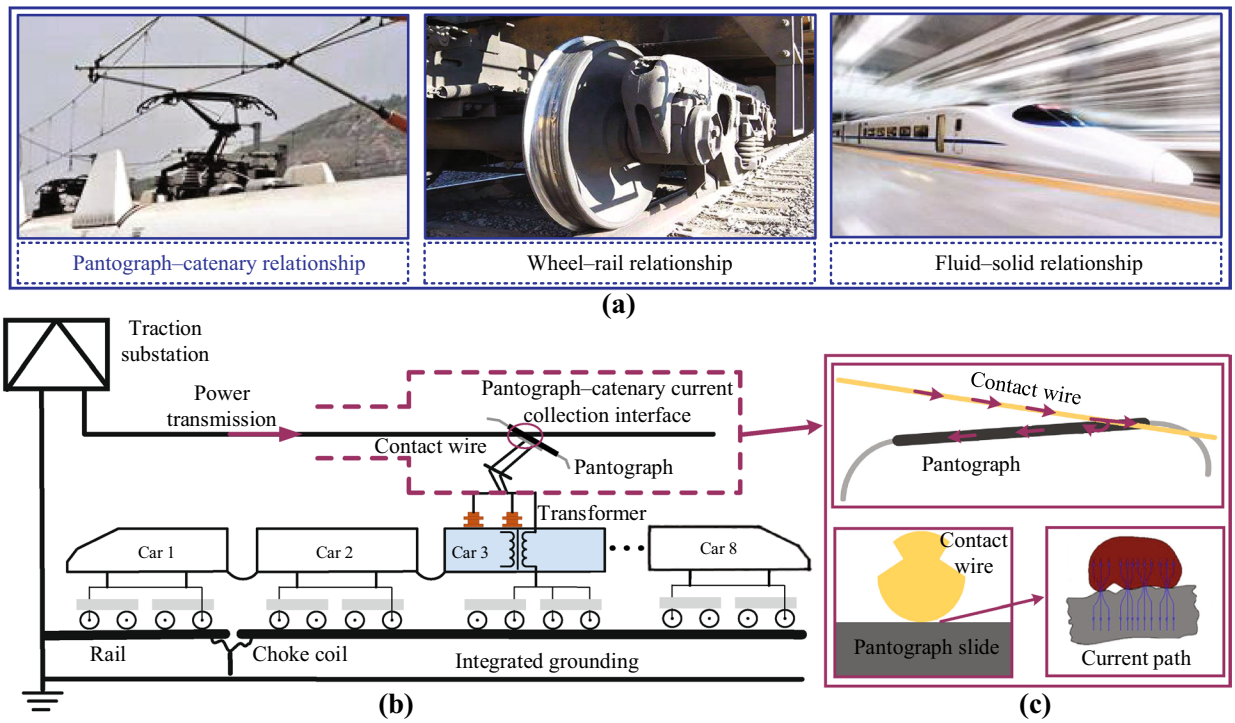

Fig. 1 **a** Three basic relationships of high-speed railway, **b** the pantograph–catenary system, and **c** the current collection process of electrical contact system

reliably. Figure 1c shows the electrical contact current collection process of the pantograph–catenary system. With the increase of train velocity, the mechanical–electrical coupling vibration between the pantograph and catenary is significantly intensified, resulting in the contact loss phenomena occurring between the contact wire and the pantograph slide, which might trigger arc. The arc ablation, friction and wear, vibration and mechanical impact tend to bring serious threats to the pantograph–catenary electrical contact interface, leading to the failure of the pantograph–catenary electrical contact system, which will seriously affect the safe running of trains and even cause the trains to stop running. The bottleneck restricting the safe and stable current collection of pantograph–catenary electrical contact systems consist mainly in three aspects: Firstly, there is a lack of pantograph slide materials with high performance in wear resistance, ablation resistance and impact resistance. Secondly, with the increase of speed, the matching of pantograph slide and contact wire deteriorates and the following performance of the pantograph–catenary system gets worse. Thirdly, there is a lack of effective equipment for online detection and early warning of pantograph–catenary system.

With the rapid development of the economy, the ultra-high-speed train is the development goal of high-speed railway. In pursuit of higher operational velocity and stronger carrying capacity, the matching condition of the pantograph–catenary electrical contact system must be improved to provide the outstanding transmission capability. Moreover, the high-speed railway tends to face more complex environments, along with the expansion of commercial railway. Some environmental uncertainty tends to bring more technique difficulties to the construction of railways, in terms of the geographical and climate elements. In addition, with the change of global climate, extremely harsh environments of different types and degrees may appear in different countries over the world. Take the climate and environmental factors in some typical countries with advanced high-speed train technology for example: earthquakes and typhoons sometimes occur in Japan [3–5], heavy rainfall occasionally occurs in Europe [6–15], and strong snowstorms usually occur in Russia [16, 17], as shown in Fig. 2. The operation and maintenance of existing high-speed railways and the development of future high-speed railways must face these complex environmental elements. China has a vast territory and different environments in different regions, such as high altitude and strong sandstorms in the west, rain and lightning in the south, typhoons in the southeast, and severe cold in the northeast [18–21], as shown in Fig. 3. In recent years, many achievements have been made in the construction of China's high-speed railways in complex environments, such as the Harbin–Dalian railway line in extremely cold environment, the Xining–Chengdu railway line with the largest slope grade, the Hainan Circum-island railway in lightning prone environment and the Lanzhou–Wulumuqi railway line in strong sandstorm environment, as shown in Fig. 4. China's experience in construction and operation of high-speed railways in these extremely complex environments may provide reference and guidance for the development of high-speed railways all over the world.

As the unique entrance of power transmission, the pantograph–catenary system plays a critical role in maintaining the reliability and robustness of the current collection process for high-speed trains. This paper first reviews the development of high-speed railway pantograph–catenary system. Then, the evolution process of catenary, pantograph and pantograph slide are summarized, and the detection and evaluation methods of pantograph–catenary system are reviewed. At last, challenges brought by the future development of high-speed railway to pantograph–catenary system are analyzed, and outlooks on the development of pantograph–catenary system in the future are discussed.

2 Development of the pantograph–catenary electrical contact system

2.1 Prototypes of pantograph–catenary system

2.1.1 The electrified railway and pantograph–catenary system in the world

In 1879, Ernst Werner von Siemens exhibited the world's first electric locomotive with a maximum speed of 13 km/h at the World Trade Fair in Berlin, of which traction power and voltage are 2.2 kW and DC 150 V, respectively, as shown in Fig. 5a. In 1881, Siemens laid the first tram line in Berlin, but people or animals will suffer electric shock when they cross the track; therefore, the method of supplying power to the train through two tracks is inappropriate. In order to solve this problem, the method of erecting two contact lines above the track was adopted in 1882, as the bus bar was hung on the contact line. However, the bus bar was often derailed due to the drag of the flexible cable, so it might not be a reliable power supply mode. Until 1889, Siemens firstly proposed an arcuate current collector, as shown in Fig. 5b, as the current collector supplies current from the catenary to the traction unit and returns through the track. This power supply mode is not only a breakthrough in train current collection technology but also a prototype of modern pantograph–catenary system [22].

2.1.2 The electrified railway and pantograph–catenary system in China

In 1961, the Baoji–Fengzhou railway line was put into operation (Fig. 6) with the 25 kV traction power of 50 Hz frequency, marking that China's railway entered the era of electrified railway [23]. Academician Cao Jianyou of

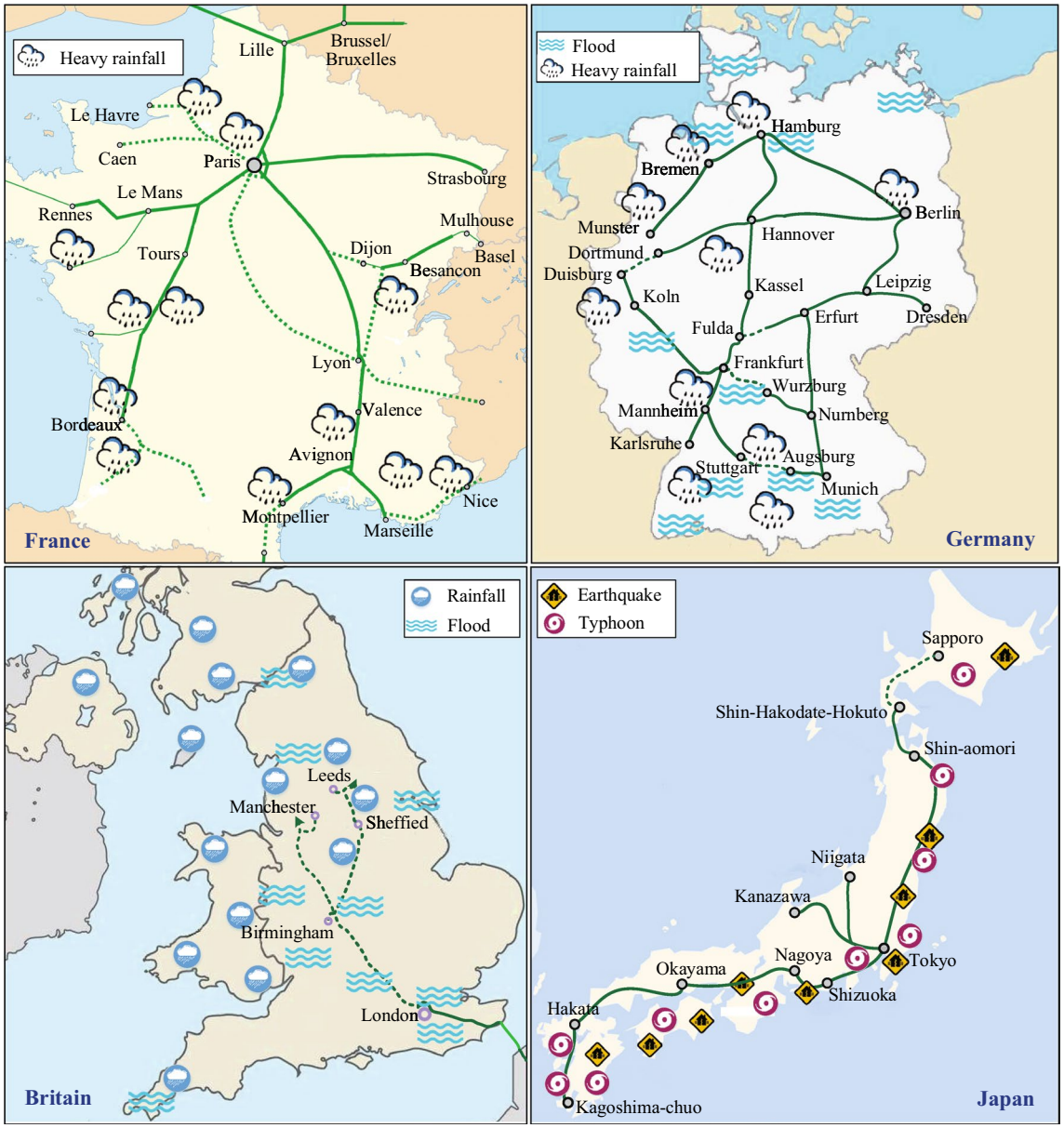

Fig. 2 Complex environments in different countries (the green lines represent high-speed railway lines)

Southwest Jiaotong University, as the main decision-maker and arguer of China's traction power supply system, has made important contributions to China's electrified railway power supply system and the development of the electrified railway. At the initial stage of the electrified railway, the trains are mainly equipped with Soviet Union ДЖ-5 pantographs, which were the basis for the formulation of the design scheme and parameter selection of the catenary in the Baoji–Fengzhou railway line. The catenary adopted elastic chain suspension and simple chain suspension, with large spans, which became the basic form of China's electrified railway pantograph–catenary system.

2.2 Development of pantograph–catenary system

2.2.1 Catenary

2.2.1.1 The structure of the catenary The catenary is mainly composed of contact suspension, support device, positioning device, pillar and foundation [24], as shown in Fig. 7.

The contact suspension includes contact wire, dropper, messenger wire, connecting parts and insulators. The contact suspension is installed on the pillar through the support device, and its function is to transmit the electrical energy obtained from the traction substation to the train.

Fig. 3 Complex environments in China

The contact suspension can be divided into two types—simple contact suspension and chain-shaped suspension, in which the chain-shaped suspension can be divided into composite chain-shaped suspension, elastic chain-shaped suspension and simple chain-shaped suspension. For simple contact suspension, there is only contact wire without continuous messenger wire. The remarkable characteristic of chain suspension is that the contact wire is hung on the messenger wire through the dropper [25].

The support device includes cantilever, horizontal tie rod, suspension insulator string, rod insulator and other equipment. The function of the support device is to support the contact suspension and transfer its load to the pillar [26]. The positioning device includes a positioning tube and a locator. Its function is to fix the position of the contact wire, make the contact wire within the running track of the pantograph slide, ensure that the contact wire is not separated from the pantograph, and transmit the horizontal load of the contact wire to the pillar [27].

The pillar and foundation are used to bear all the weight of the contact suspension, support and positioning device, and fix the contact suspension at the specified position [28]. The pillar and foundation of the catenary are generally made of steel pillars and reinforced concrete. The steel pillars are fixed in the foundation made of reinforced concrete below, and the foundation bears all the weight of the pillars and ensures their stability.

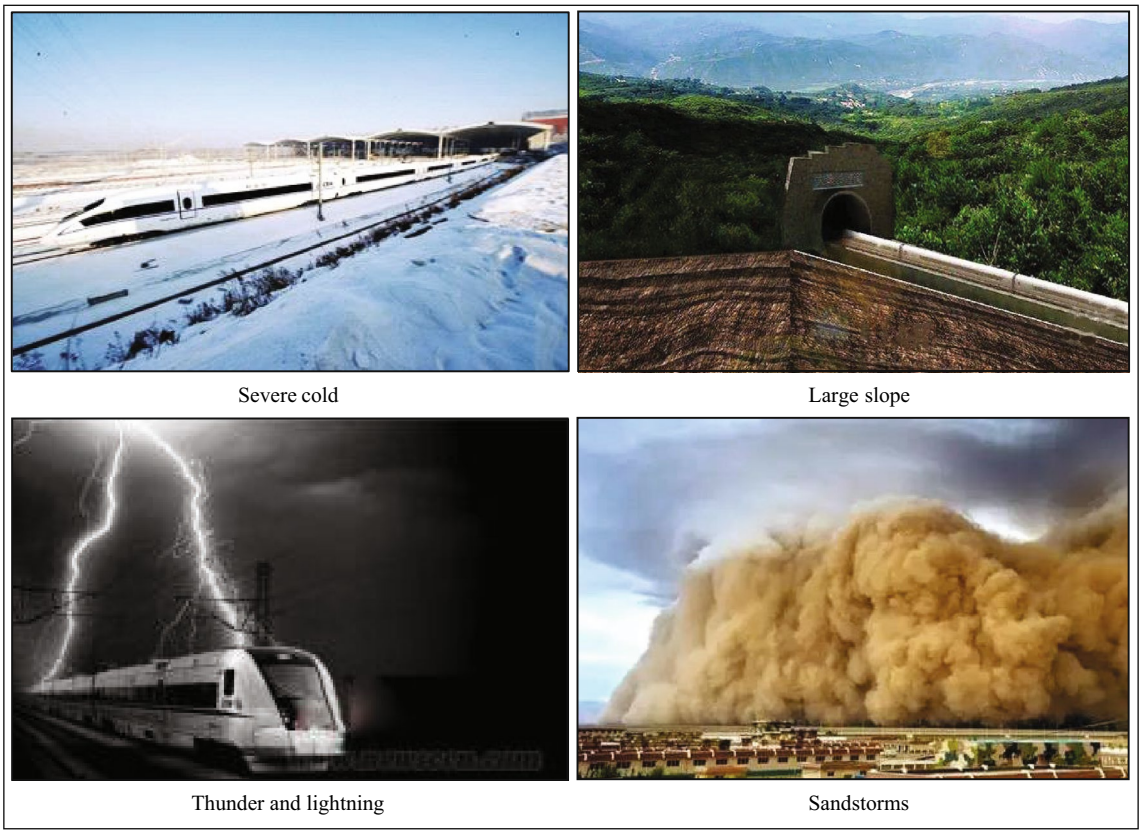

Fig. 4 High-speed railways of China in harsh environments

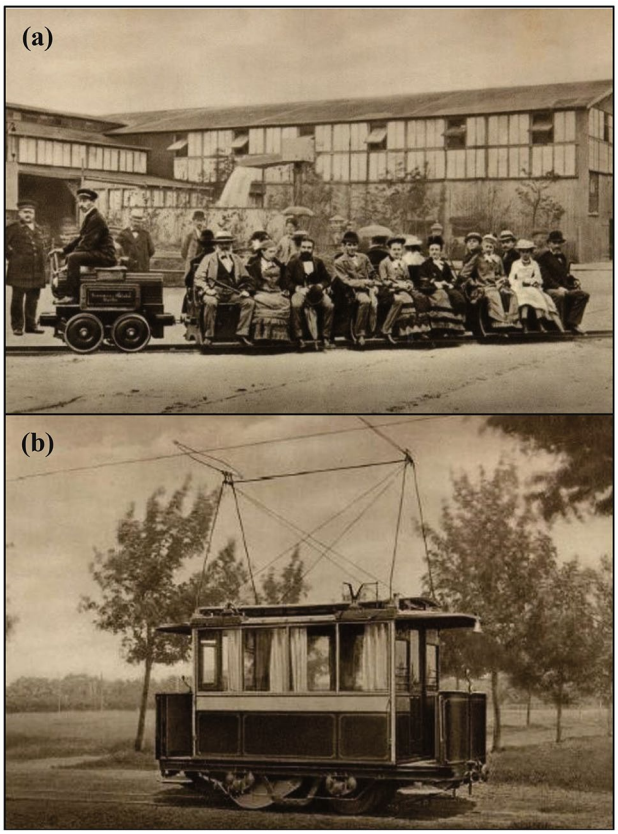

Fig. 5 Prototype of electric locomotive and pantograph–catenary system: **a** the electric locomotive; **b** arcuate current collector

2.2.1.2 Development of the catenary Since the Shinkansen started operation in 1964, the catenary has been developed for more than 50 years, and its suspension type has also been continuously improved. The general trend of catenary development and evolution all over the world is the same, that is, from a complex and high-cost catenary structure to a simple and low-cost catenary structure. The

Fig. 6 The electric locomotive on Baoji–Fengzhou railway line

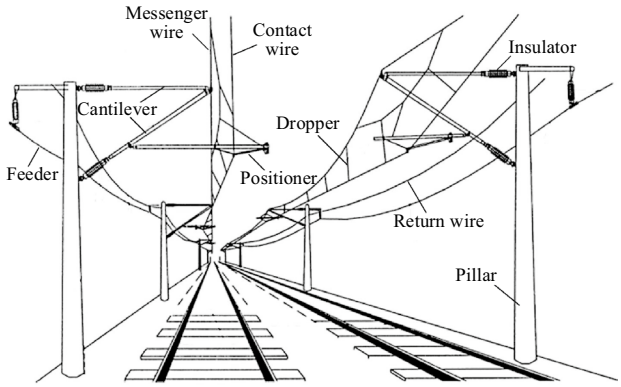

Fig. 7 The configuration of the railway with catenary

earliest catenary was a composite chain-shaped suspension catenary. Due to its complex structure, high cost and difficult maintenance, it was gradually replaced by the elastic chain-shaped suspension catenary. The catenary with elastic chain-shaped suspension has simple structure and high stability, which can meet the current collection requirements of trains running at high speed. In recent years, the structure of the catenary has been further simplified, and the simple chain-shaped suspension catenary with low cost and simple maintenance is widely used all over the world.

2.2.2 Pantograph

In the electrified railway, the pantograph is the key equipment for the train to obtain electric energy from the catenary, and its structure is an important factor affecting the current collection quality. Relevant research shows that when the train speed reaches 200 km/h, the mechanical collision between pantograph and catenary is more violent, and the arcing is more frequent, resulting in serious damage to the pantograph–catenary system. Therefore, it is of great significance to study pantographs with excellent performance to promote the development of high-speed railway [29].

2.2.2.1 The structure of the pantograph The pantograph is mainly composed of pantograph head, frame, under frame and transmission system, as shown in Fig. 8. The pantograph head is an important part of the pantograph, which mainly includes slide plate, pantograph angle and pantograph head support device. The slide plate is a current collection device fixed on the top of the pantograph with the slide plate bracket, which is a replaceable consumable. The pantograph angle is an arc part installed at both ends of the pantograph head. Its main function is to ensure that the pantograph passes through the overhead crossover of the catenary smoothly. In addition, in order to prevent the pantograph angle from discharging to the roof when work-

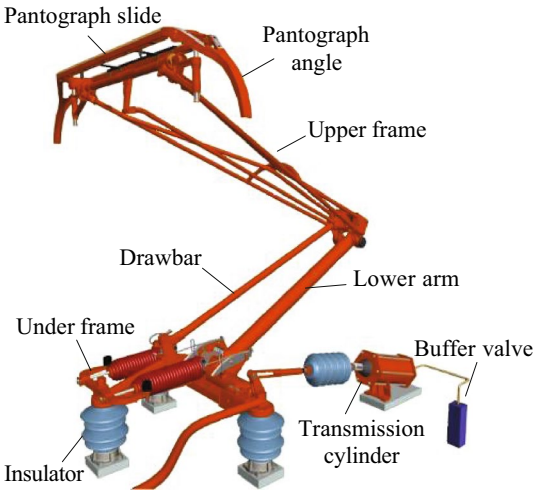

Fig. 8 The structure of pantograph

ing with electricity at a lower height, the pantograph angle must be made of insulating material. Pantograph head support device is one of the key components affecting the performance of pantograph. Its function is to ensure smooth contact between slide plate and contact line and is generally made of materials with high strength and light weight [30].

Generally, the frame types include double-arm and single-arm frames. The double-arm frames include the four-wrist diamond double-arm frame and the two-wrist diamond double-arm frame. The four-wrist diamond double-arm frame is composed of four arms, and each arm includes two parts: the upper arm and the lower arm, which are symmetrically arranged in front and back, left and right. This type of frame has the advantages of high strength and good stability, but it has the disadvantages of high cost, large weight, complex structure and difficult adjustment. Later, the four-wrist diamond frame was improved, and the lower frame was changed from the original four arms to two arms, while the upper frame remained unchanged, so it was called two-wrist diamond double-arm frame. Compared with the four-wrist diamond double-arm frame, the two-wrist diamond double-arm frame is simpler in structure, lighter in weight, and less difficult to adjust. The double-arm frame is gradually phased out because of its complex structure, heavy weight and high maintenance costs, and displaced with the single-arm frame. The structure of the single-arm frame is only half of that of the two-wrist diamond double-arm frame, which has the advantages of simple structure, small overall size, light weight, easy adjustment and good dynamic characteristics. Therefore, the single-arm pantograph is widely used in modern electrified trains [31, 32].

The underframe is the base fixed to the pantograph frame and installed on the supporting insulator of the pantograph at the top of the train. It is usually made of section steel, steel pipe or casting. Generally, the underframe is required to have strong rigidity to avoid the deformation of the frame during handling or installation, which will affect the performance of the pantograph [33].

The transmission system is used to raise or lower the pantograph, which mainly includes pantograph raising spring, pantograph lowering spring and transmission cylinder. When the pantograph is raised, the compressed air enters the transmission cylinder evenly through the electro-pneumatic valve, the cylinder piston compresses the pantograph lowering spring in the cylinder. At this time, the pantograph raising spring pulls the lower arm to raise the upper frame and the pantograph head until the slide plate contacts the contact line. When the pantograph is lowered, the compressed air in the transmission cylinder is discharged quickly. The pantograph lowering spring overcomes the force of the pantograph raising spring to make the pantograph lower quickly [34].

2.2.2.2 Development of the pantograph With the development of electrified trains, the pantographs have been constantly refined. Although the development histories of electrified railways in various countries are different, the development of pantographs worldwide can be summarized as an evolution process from double-arm pantographs with complex structure and high weight to single-arm pantographs with simple structure, low weight, flexibility and reliability.

Initially, four-wrist diamond-shaped double-arm pantographs were used in the early stage of high-speed railway operation, but they were eliminated due to their complex structure and the large aerodynamic noise generated when the trains were running at high speed. Japan then successfully developed a T-type pantograph, which has a simple structure but a high cost, so they are no longer used at present. Subsequently, Japan developed PS207 and PS208 single-arm pantographs, and in 2011, the maximum running speed of E5 series high-speed trains with PS208 single-arm pantographs reached 320 km/h [35]. France, Germany and China established high-speed railways after Japan, and all of them use single-arm pantographs, which are small, lightweight and reliable and have excellent aerodynamic performance.

The pantograph plays a pivotal role in the quality of the pantograph–catenary current collection. In order to meet the safe and stable energy transmission of ultra-high-speed trains in the future, it is necessary to continuously develop novel pantographs with better comprehensive performance, simple structure and light weight. In addition, improving the matching performance between pantograph and catenary is also a key task for the development of future high-speed railway pantograph–catenary systems.

2.3 Pantograph–catenary system in different countries

Japan, France, Germany and China are the representatives with developed high-speed railway network in the world, and their high-speed railway pantograph–catenary systems have experienced different development processes.

2.3.1 The pantograph–catenary system in Japan

In 1964, Japan built the world's first high-speed railway—Tokaido Shinkansen, with a running speed of 210 km/h [36], as shown in Fig. 9. The traction power supply system of Tokaido Shinkansen adopts AC 25 kV, 50/60 Hz. The opening of the Shinkansen raised the average speed of Japanese trains from 64 to 210 km/h, which brought the development of electric locomotive and pantograph–catenary systems into a new era.

Figure 10 shows the development process of Shinkansen pantograph–catenary system in Japan. At the initial stage of the opening of Shinkansen, the pantograph–catenary system was composed of PS200A pantograph and a complex chain suspension catenary with elastic combined suspension string. However, the elastic combined suspension string would increase the vibration of the catenary, and the pantograph–catenary electric contact system is poorly matched. Therefore, the Japanese Shinkansen pantograph–catenary system was replaced by a heavy-duty complex chain suspension catenary with a Y-shaped elastic sling. The multi-pantograph current collection model was adopted. However, in the long-term operation, it was found that the wear of the pantograph–catenary system was serious, and the contact wire needed to be replaced once every 4–5 years. In order to solve this problem, Japan optimized the pantograph–catenary system from multi-pantograph current collection to double pantograph current collection. The pantograph gradually became lighter (such as T-shaped pantograph and V-shaped single-arm pantograph), and the catenary suspension mode was changed to the simple chain suspension. While the train running speed was improved, and the service life of the pantograph–catenary system was also extended.

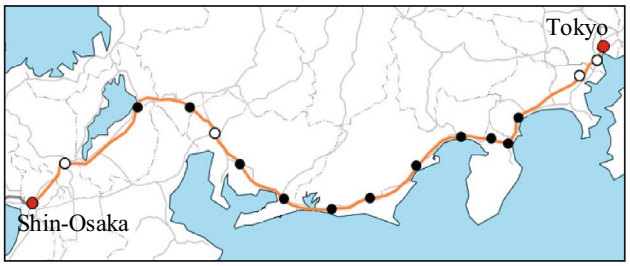

Fig. 9 Tokaido Shinkansen railway line

The seismic design of the catenary is a typical feature of the Japanese Shinkansen pantograph–catenary system. The purpose of seismic design is to prevent the collapse of catenary equipment caused by earthquakes. The seismic design policy considers the dynamic interaction between pillars, catenary suspension, catenary equipment, and supporting civil structures. The continuous development and improvement of the seismic design of Shinkansen in Japan provide an important reference for the construction of electrified railways in earthquake-prone countries in the world.

2.3.2 The pantograph–catenary system in French

In 1981, the first high-speed railway in France, namely TVG, was put into operation, becoming the second country with high-speed railway after Japan, opening the era of high-speed railways in continental Europe. The TGV high-speed railway adopts a traction power supply system of AC 25 kV,

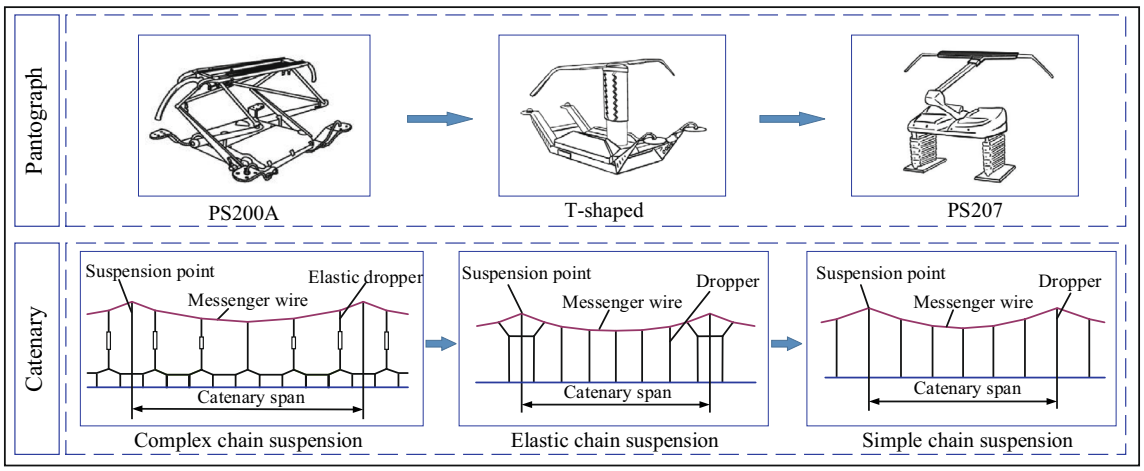

Fig. 10 Development of Japanese Shinkansen pantograph–catenary system

50 Hz, and the trial operation speed reached the world record of 380 km/h at that time, breaking the concept of the traditional railway operation speed.

The TGV train is one of the fastest high-speed trains in the world. In 1990, TGV set a world record of 515.3 km/h on the Atlantic branch line [37], which is the first time in human railway history to exceed the speed of 500 km/h. In 2007, the maximum speed of the TGV-V150 test train reached 574.8 km/h [38], which created the world's first wheel–rail railway speed, as shown in Fig. 11.

Fig. 11 The TGV-V150 test train

Figure 12 shows the development process of the TGV pantograph–catenary system. TGV pantograph–catenary system of the southeast line in France is composed of the AMDE pantograph and the elastic chain suspension catenary. In order to meet the needs of improving the running speed of high-speed railway, the French high-speed railway has carried out many optimizations on the pantograph–catenary system. In 1991, France developed the CX pantograph with excellent performance matching with the catenary with a simplified structure. The simple chain catenary was adopted in the construction of the high-speed railways after the Southeast line [39].

The prominent feature of French TGV is the pursuit of speed. In order to achieve the goal of higher speeds, the TGV train always adopts the mode of power centralized configuration and articulated vehicle connection. With the continuous improvement of the TGV pantograph–catenary system, its pantograph has gradually realized lightweight (e.g., the CX series pantograph has the smallest pantograph head size in the world), and the catenary has evolved from the elastic chain suspension to the simple chain suspension.

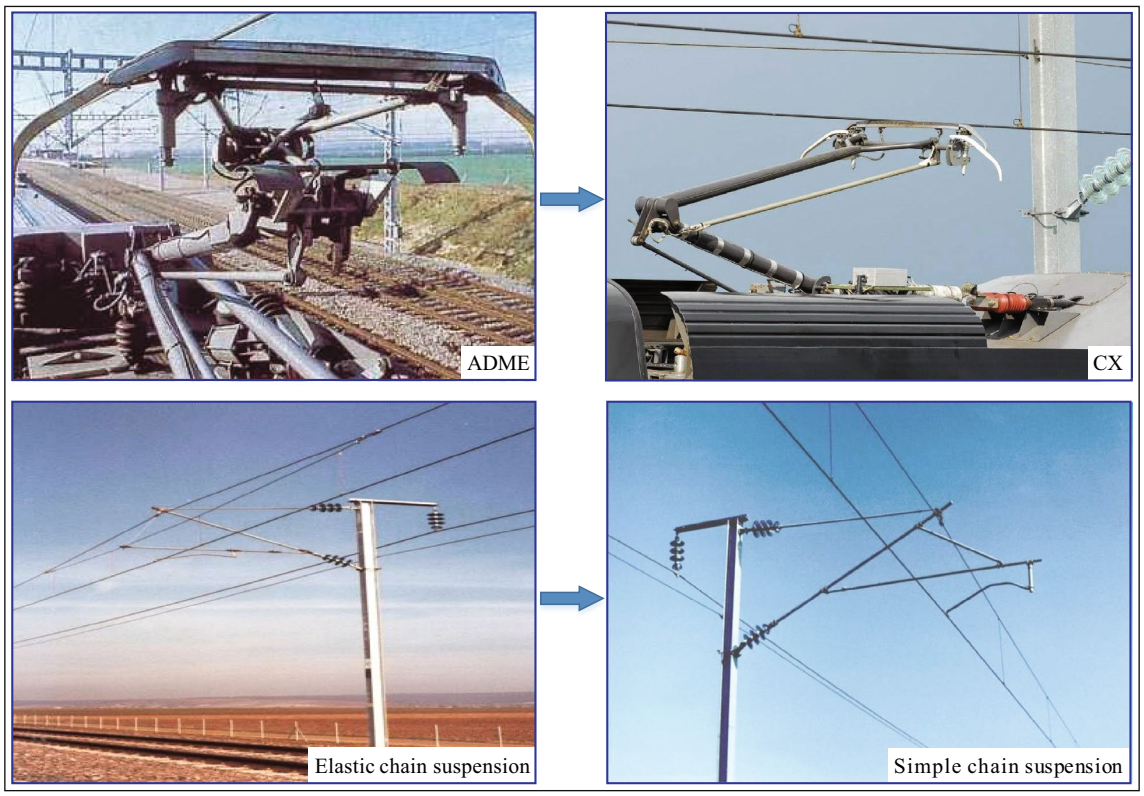

Fig. 12 Development of French pantograph–catenary system

Table 2 Main technical parameters of ICE trains

Train	Power (kW)	Operation start year
ICE1	4800	1991
ICE2	4800	1992
ICE3	8000	2000
ICE4	9900	2017

2.3.3 The Pantograph–catenary system in German

In 1991, the German high-speed railway began to operate with a maximum speed of 250 km/h. ICE is one of the most reliable, advanced, and comfortable high-speed railways in Europe. The German electrified railway adopts a traction power supply system of AC 15 kV, 16.67 Hz. ICE trains are characterized by high power, and their main technical parameters are shown in Table 2.

The German ICE pantograph–catenary system uses a DSA350SEK pantograph with a large contour bowhead and long-span elastic chain suspension catenary (such as Re160 and Re200), as shown in Fig. 13a. German high-speed railway sector has conducted in-depth research on the pantograph–catenary system and made many achievements. Figure 13b shows the development process of the German catenary. In the mid-1970s, Germany developed the Re250 catenary (suitable for 250 km/h) on the basis of the Re200 catenary [40]. In the 1990s, Re330 catenary (applicable to 300 km/h) was developed, and its speed target value could reach 400 km/h [41, 42]. After many years of development, the long-span elastic chain suspension catenary has become the best choice of German high-speed railways and has been applied until now.

A remarkable feature of the German high-speed railway is that the power supply system adopts AC15kV and 16.67 Hz. The advantages of this single-phase low-frequency AC system are small voltage loss and low power loss. Another feature of the German high-speed railway is safety, comfort, and high economy. The pantograph with a large bowhead size is adopted, and the long-span elastic chain suspension is used to reduce the elastic unevenness of the catenary. The large outline pantograph matching with the long-span catenary can effectively improve the economy and reliability of the German railway pantograph–catenary system.

2.3.4 The pantograph–catenary system in China

The development of China's high-speed railways has experienced a brilliant process from scratch, from manufacturing to creation, and from introduction to going out. In 2007, as the first high-speed railway in China, the Suining–Chongqing railway line was officially put into operation, with a design speed of 200 km/h, which laid a theoretical foundation and

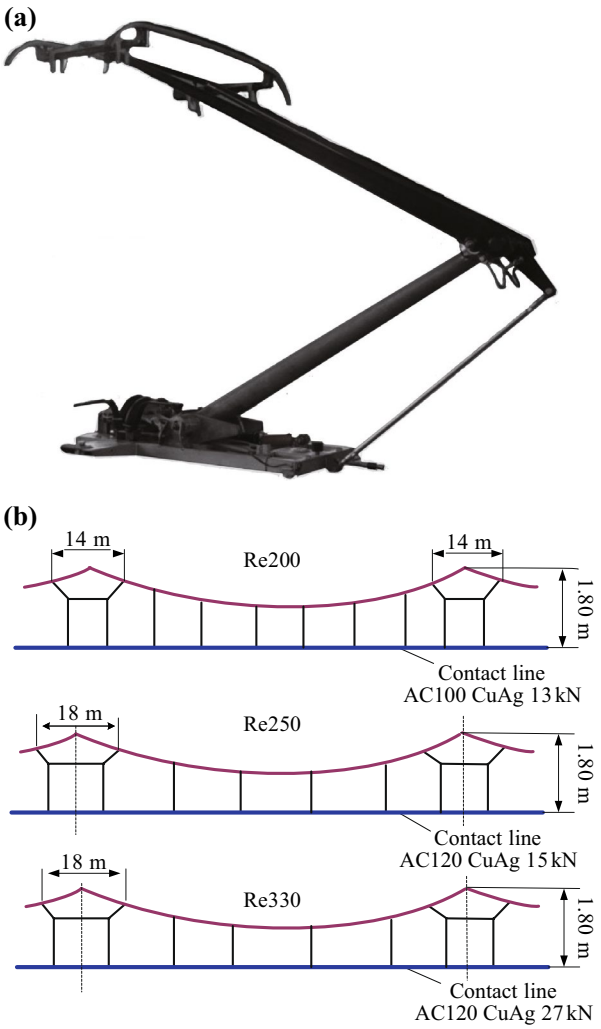

Fig. 13 Development of German pantograph–catenary system: **a** DSA350SEK pantograph; **b** development of German catenary

technical reserve for China's large-scale high-speed railway construction. In 2008, China's first high-speed railway with a design speed of 350 km/h, the Beijing–Tianjin Intercity High-speed Railway, was put into operation, whose operation speed is the fastest in the world at that time. In 2009, Wuhan–Guangzhou high-speed railway was put into operation, which has become a sign that China has officially entered the era of high-speed railway [43]. In 2010, the CRH380AL EMU using the DSA380 pantograph set a new record for the operating train test speed of 486.1 km/h on the Beijing–Shanghai high-speed railway, as shown in Fig. 14.

The development of pantograph–catenary system for China high-speed rail has gone through the process of introduction, absorption, and re-innovation. Figure 15 is the development process of the catenary and pantograph. In the early stage of China's high-speed railway construction, the pantograph–catenary system adopted the imported

DSA200 pantograph and Re200C elastic chain suspension catenary. During the sixth speed increase of China Railway in 2007, the DSA250 pantograph was widely used [44]. The design speed of this pantograph is 250 km/h, which is suitable for various electric locomotives and electric multiple units (EMUs) of corresponding speed grades. With the continuous improvement of train speed, pantograph and catenary are also developing and improving. In 2008, the Beijing–Tianjin intercity railway was put into operation. In order to meet the high-speed current collection requirements of EMUs, the pantograph–catenary system adopted an SSS400 + pantograph and a simple chain suspension catenary. The SSS400 + pantograph has been localized through a process of re-innovation, and the model after localization was TSG19. In 2011, the Beijing–Shanghai railway line was put into operation, and its catenary also adopted the simple chain suspension. The CRH380BL train running on the Beijing–Shanghai railway line began to use the CX-NG pantograph with excellent performance. In 2017, China's self-developed standard EMU train 'Fuxing' started operation. 'Fuxing' adopted the CX-G1030 pantograph, and some components of the pantograph–catenary system were localized [45, 46]. In fact, China is taking the lead in research and development of high-speed railways.

Fig. 14 The CRH380AL test train

2.3.5 *Other typical pantograph–catenary systems*

In addition to the above-mentioned, the pantograph–catenary system of Sweden's X2000 high-speed pendulum train is also a typical one [47], as shown in Fig. 16. The catenary of the pendulum train pantograph–catenary system adopts simple chain suspension, and the pantograph adopts a WBL88-X2 type pantograph. The WBL88-X2 pantograph can be controlled laterally on a curved track to realize reverse inclination relative to the vehicle body, which can reduce pantograph–catenary system vibration and improve current collection quality. The adoption of high-speed pendulum trains is a significant feature of Swedish high-speed railways, which can increase the passing speed of trains by 30% to 40% in the curved section. At the same time, the tilt of the car body offsets 70% of the centrifugal force felt by the passengers, making the passenger experience more comfortable.

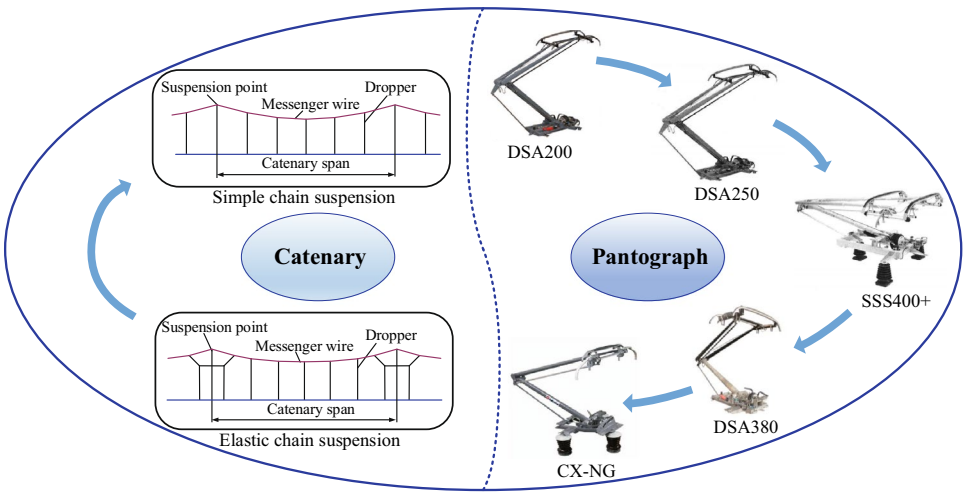

Fig. 15 Development process of catenary and pantograph in China

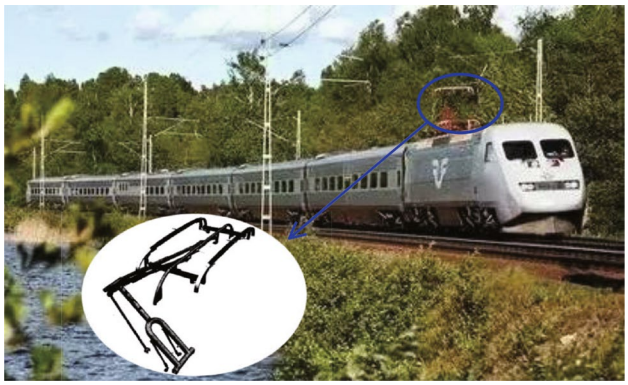

Fig. 16 Sweden's X2000 high-speed pendulum train with the WBL88-X2 pantograph

3 The component evolution of pantograph–catenary system

3.1 Contact wire

Contact wire is an important part of catenary, which transmits electrical energy to the electric locomotive through pantograph slide. Contact wire is generally built in zig-zag to reduce the wear on pantograph slide. When the train is running at a high speed, the contact wire has to face the extreme working environment such as vibration shock, temperature difference, environmental corrosion, mechanical friction, and arc ablation [48]. Its material properties directly affect the current collection quality and operation safety of the train. There are many types of electrified railway contact wires, which are mainly classified into pure copper contact wires and copper alloy contact wires according to the material [49].

3.1.1 Pure copper contact wire

Pure copper has excellent electrical conductivity, thermal conductivity and corrosion resistance, but it has low strength, low softening temperature and poor heat resistance. The pure copper contact wire is easily broken, causing the pantograph–catenary system to fail. Therefore, pure copper contact wire cannot meet the requirements of high-speed and heavy-haul railways, it is generally only suitable for ordinary railway with speeds lower than 200 km/h [50]. At present, it is gradually replaced by copper alloy contact wire.

3.1.2 Copper alloy contact wire

The metal elements doped with copper alloy mainly include Ag, Sn, Cr, Mg, and Zr. Due to the addition of metal elements, the mechanical properties, softening resistance and wear resistance of copper alloy contact wire are greatly improved compared with pure copper.

Copper–silver alloy contact wire usually refers to copper as the main material, containing about 0.1% silver element. Ag and Cu are homologous elements with similar electronic structures, so copper–silver alloys can achieve an electrical conductivity of 96% IACS or more. Copper–silver alloy contact wire is used in Re250 catenary in Germany, and the train speed can reach 250 km/h. However, since Ag and Cu are cognate elements, the solid solution strengthening effect is not prominent, and the improvement of mechanical properties of copper–silver alloy at room temperature is limited, which is about 370 MPa. At present, the copper–silver alloy contact wire produced in China has reached a high level and can be used for high-speed railways below 300 km/h.

Copper–tin alloy contact wire is made by adding 0.3% tin element to copper. Compared with the copper–silver alloy wire, the copper–tin alloy contact wire has advantages of simple manufacturing process, high yield and low price. In 1997, Japan achieved the goal of 300 km/h by using the copper–tin alloy contact wire [51]. The copper–tin-120 contact wire developed in France and tested in a catenary with a speed of 300–350 km/h has a tensile strength of 537.5 MPa and an electrical conductivity of 70% IACS. The copper–tin alloy contact wire has high strength, high softening temperature and appropriate electrical conductivity, and its comprehensive performance is better than that of the copper–silver alloy contact wire [52].

Copper–magnesium alloy contact wire is a milestone wire after copper–tin alloy contact wire. It has the characteristics of high tensile strength, high wear resistance, high temperature softening resistance, moderate electrical conductivity, etc. It is mainly used in high-speed railway catenary with a speed of more than 300 km/h [53]. Copper–magnesium alloy contact wire was first developed by German Railway Company (DBAG), with a tensile strength of 490 MPa and an electrical conductivity of 62% IACS. It was applied in Re330 catenary, and the speed could reach 330 km/h. China has begun to develop copper–magnesium alloy contact wire since 1990s. In 2002, copper–magnesium alloy contact wires were successfully applied to Qinhuangdao–Shenyang high-speed railway. Since then, copper–magnesium alloy contact wires have been mostly used in lines with a design speed of 300 km/h and above in China.

Copper–chromium–zirconium alloy contact wire is a copper alloy product strengthened by heat treatment. It has high tensile strength and significantly improved electrical conductivity compared with contact wires made of copper–tin alloy and copper–magnesium alloy. The Chinese TB/T2809-2017 standard requires that the tensile strength of copper–chromium–zirconium contact wire shall not be less than 560 MPa and the electrical conductivity shall not be less than 75% IACS. In 2010, the 220 km pilot test section

of Beijing–Shanghai high-speed railway set a world record speed of 486.1 km/h with copper–chromium–zirconium contact wire for high-speed railroad operation test. Copper–chromium–zirconium alloy contact wire material has high strength, good electrical conductivity and high temperature softening resistance. It can be applied to high-speed railway above 350 km/h and has broad application prospects. However, its production process is totally different from that of ordinary copper–silver, copper–tin and copper–magnesium alloy contact wires. It requires multi-pass and long-time heat treatment, and due to its complex process, the production cost is higher than that of other contact wires [54].

Table 3 shows the key performance parameters of different types of contact wires. Facing the development direction of high-speed railways to higher speed, contact wire materials are required to have better comprehensive properties. For the existing types of contact wires, it is necessary to optimize the alloy composition design, optimize the process flow of copper alloy wire blank, improve the reliability of products, and reduce the cost. Meanwhile, it is necessary to strengthen the research and development of advanced production technology and processing equipment.

3.2 Pantograph slide

As the key current collection part of the high-speed train, the pantograph slide is installed on the top of the train. It directly contacts with the contact wire and gets electric energy to provide traction power for the stable operation of the locomotive [57, 58]. The current collection quality of the pantograph–catenary system determines whether the train can obtain sufficient traction power to run safely and reliably [59]. The performance of the slide plate material used in the pantograph directly determines the quality of the current collection. In addition, the pantograph slide is exposed to the ambient environment, so it would face mechanical impacts, arc erosion, and friction continuously during the running of trains [60–62]. Therefore, the design of the pantograph slide has very strict requirements which include sufficient impact resistance, high electrical conductivity, good abrasion and ablation resistance, excellent self-lubrication, and low wear property against the contact wire. The general requirements for the pantograph slide material are shown in Fig. 17.

With the development of high-speed and heavy-haul electrified railway, a higher requirement for the performance of the pantograph slide materials is needed. Research on the pantograph slide, especially on its materials, has been studied extensively all over the world. Since the 1920s, countries like Japan, France and Germany have done a lot of studies on the pantograph, laying a solid foundation for the development of pantograph slide materials.

The development of pantograph slide materials has experienced different stages, including metal slide plate, pure carbon slide plate, powder metallurgy (P/M) slide plate, metal impregnated carbon slide plate, and composite slide plate [63–65]. The development of the pantograph slide corresponding to trains with different speed levels is shown in Fig. 18. Since the 1960s, China has made remarkable achievements in pantograph slide materials. In 1961, China's the first electrified railway, namely Baoji–Fengzhou railway was put into operation with a maximum running speed of 70 km/h, where the mild steel pantograph slide was mainly used. This kind of pantograph slide has the advantages of high mechanical strength, low resistivity, low cost, and long service life. However, the lubricity of this pantograph

Table 3 The key performance parameters of different types of contact wires [49, 50, 55, 56]

Materials	Tensile strength (MPa)	Electrical conductivity (%IACS)	Country	Speed ($km \cdot h^{-1}$)
Cu	350–360	97.5	Most countries (before 2013)	≤200
Cu–Ag	353	96.5	China	≤250
	350	96.5	Germany	
Cu–Sn	538	73.8	China	≤350
	420	85	Japan	
	537.5	77.6	France	
Cu–Mg	490	62.1	Germany	≥300
	524	72	China	
Cu–Cr–Zr	555.5	78.8	Japan	≥350
	569	78	China	

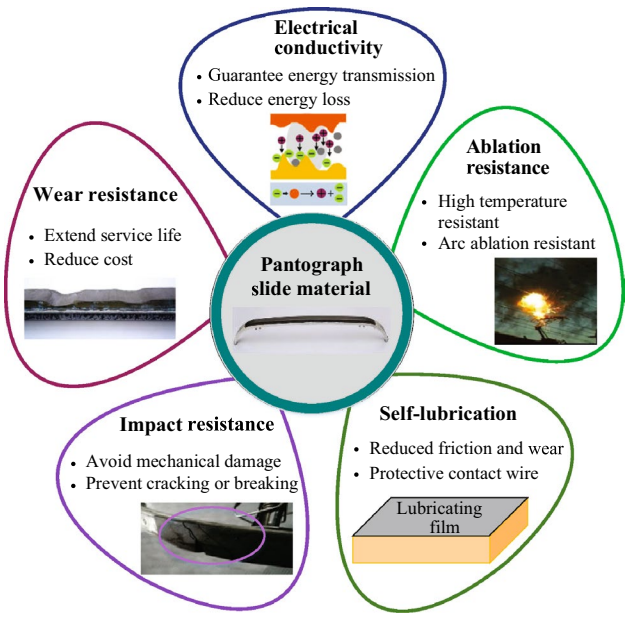

Fig. 17 Requirements for the pantograph slide material

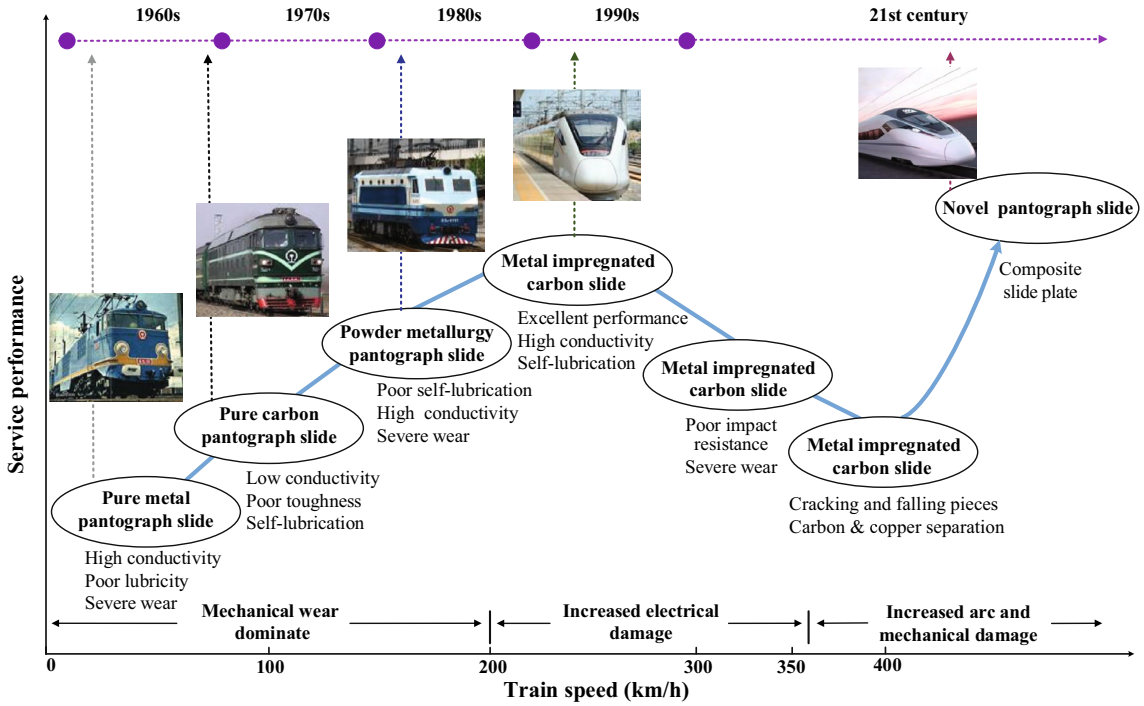

Fig. 18 Development of pantograph slide with the increase of train speed in China

is poor, which causes serious wear of the contact wire. To solve this problem, the pure carbon slide plate was developed by the Institute of Railway Sciences of China in 1967, and the mechanical wear of the contact wire was greatly mitigated.

Subsequently, as the train speed increased to 100 km/h, the pure carbon slide plate could no longer be used because of its low mechanical strength, poor impact toughness, and low service life at higher speeds. In order to solve this problem, a P/M slide plate with good impact toughness was developed, which was based on the metal (iron and copper) powder. This approach greatly reduced the wear of contact wire, and the slide plate had a better performance in wear resistance as well. It was therefore used as an ideal solution for trains on 100 km/h trunk lines.

Later on, the further increase of the train speed resulted in an increase of the contact loss rate of the pantograph–catenary and more frequent arcing phenomena during train service. Due to the loose structure and poor arc resistance, the existing P/M slide plate could no longer meet the safety requirements at 160 km/h. In the 1990s, the emerge of the metal impregnated carbon slide plate with dense structure in high-speed electric locomotive offered a promising approach to compensate for the material defects at high-speed. The metal impregnated carbon slide plate had many excellent performances such as high mechanical strength, low resistivity, low wear, easy to form a lubricating film, and strong arc extinguishing ability. It was recognized as a novel slide plate with the best adaptability to the contact wire, and got widely applied in high-speed trains running with a speed above 200 km/h. However, the existing metal impregnated carbon slide plate may not meet the requirements of ultra-high-speed trains in the future, and it is necessary to develop novel composite pantograph slides with high comprehensive performance.

3.2.1 Pure carbon slide plate

The pure copper and soft steel are mainly used as pantograph slide materials for electrified trains running at a speed below 70 km/h. However, due to the serious wear on the contact wire, the pure metal slide plate could not meet the needs of electrified railway development. Therefore, the pure carbon slide plate with self-lubricating performance replaced the pure metal slide plate and became the best choice of the pantograph slide in the low-speed stage of electrified railway.

The pure carbon slide plate is mainly composed of carbon black, pitch coke, and petroleum coke. The production process of the pure carbon slide plate is shown in Fig. 19 (green line). First, the components are made into aggregate powder, and pitch is added as the binder for the mixing process. After hot pressing and roasting, a blank is formed, and this blank is

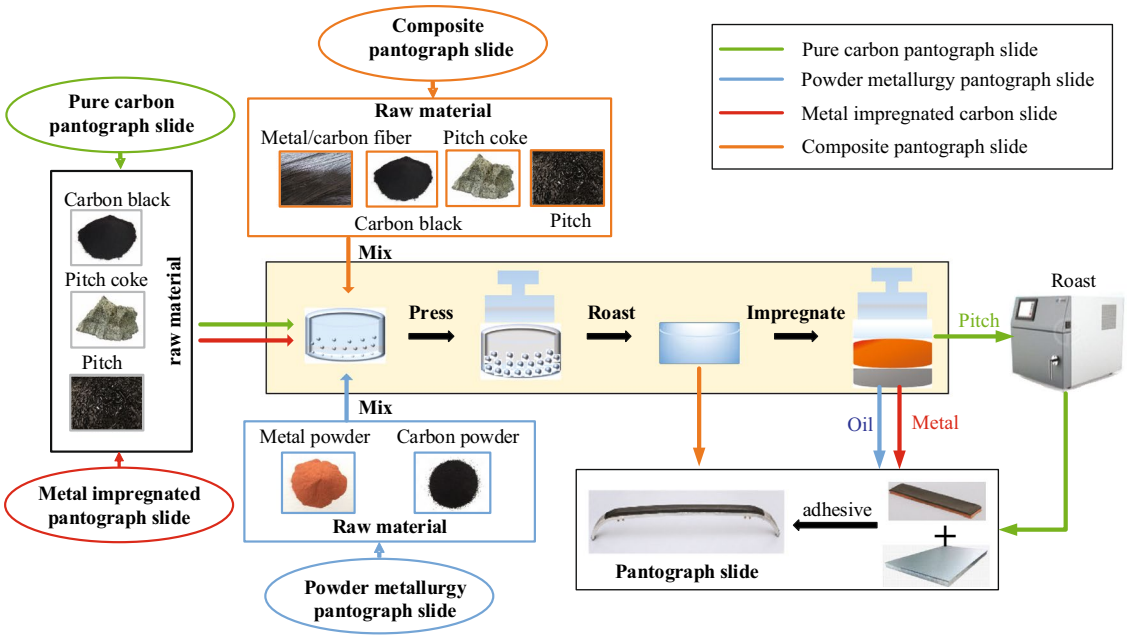

Fig. 19 The methodology of pantograph slide design and preparation

impregnated with pitch and is roasted before the preparation is complete [66].

The pure carbon slide plate has good self-lubrication, which can form a layer of lubricating carbon film on the wire when it rubs against the copper contact wire. This design effectively reduces the wire wear and prolongs the service life of the wire. Moreover, the pure carbon slide plate has advantages of low electromagnetic noise and high temperature resistance when sliding, and there is no welding problem between the carbon slide plate and the contact wire. Therefore, in the early days, the pure carbon slide plate is adopted by many countries.

Japan has been devoted to the research and development of pantograph slide materials and it began to develop and use the pure carbon slide plate in the 1920s. The pantograph slide materials were widely used in private railways in the 1940s [67]. Netherlands began to use pure carbon slide plate in 1934. In 1991, Germany ICE was founded and started to use the pure carbon slide plate with a wear rate in the range of 1.7 to 2.2 mm 10,000 km [68]. In the 1960s, the pantograph slide of electric locomotive in China adopted mild steel and pure carbon slide plate, which were gradually replaced by the pure carbon slide plate due to its excellent performances in self-lubrication and wear reduction [69, 70]. In the recent decade, China has made great progress in the research of pure carbon slide plates, and has developed pure carbon slide plate with excellent performance. Table 4 shows the key properties of the pure carbon slide plate in some representative countries.

Although the pure carbon slide plate has significant performance in mitigating the wear of the pantograph slide on the contact wire, its shortages and deficiencies become prominent as the train speed increases. Due to the low mechanical strength and poor impact resistance of pure carbon slide plate, the slide plate is easily subject to crack, block fall, or even fracture when it is sliding through the hard point of contact at a high speed. Additionally, the uneven wear of the slide plate results in an increase in the contact loss rate, which leads to a severe wear between the pantograph slide and the contact wire. In addition, pure carbon slide plates have large resistance, small collection capacity, and high temperature in the contact area, easy to

Table 4 Key parameters of pure carbon slide plate in different countries [63, 64, 66, 73, 74]

Country	Density ($g \cdot cm^{-3}$)	Hardness (HS)	Electrical conductivity ($\times 10^5$ $S \cdot m^{-1}$)	Flexural strength (MPa)	Impact strength ($J \cdot cm^{-2}$)
Germany	1.67	75	0.30	38	0.35
Japan	1.65	65	0.29	35	0.15
France	1.70	92	0.42	50	0.32
China	1.70	80	0.29	45	0.36

cause oxidation corrosion of the contact wire and shorten the service life of the pantograph and catenary. Therefore, the electrical contact current collection materials with lower resistance coefficient and higher impact toughness become the focus of researchers at higher speeds.

3.2.2 Powder metallurgy slide plate

Compared with the pure carbon slide plate, the P/M slide plate has excellent impact resistance, conductivity, arc resistance, and wear resistance. A lubricating film can be continuously formed during the operation of the P/M slide plate, which reduces the friction coefficient of the friction pair. The P/M slide plate has been studied extensively, especially in Japan and China [71, 72].

The P/M slide plate is made of metal powder (e.g., iron and copper), lubricating component (e.g., C, Pb, and MoS_2), and hard components by means of mechanical mixing, and hydroforming after hot pressing and oil immersion. Its production process is shown in Fig. 19 (blue line). The P/M slide plates can be divided into iron matrix and copper matrix plates according to its ingredients. Iron matrix slide plates are mostly used for steel aluminum wires, while copper matrix slide plates are mainly used for copper wires. The general composition of copper matrix slide plates is shown in Table 5.

The P/M slide plate was firstly developed in Japan in the 1950s. Since then, copper matrix P/M slide plate was commonly used. After the construction of Shinkansen, the iron matrix P/M slide plate was used, followed by the copper matrix P/M slide plate [73]. In 1969, the former Soviet Union developed a P/M slide plate which can be used in 1500 V DC electrified railway section. In the late 1960s, China developed a P/M slide plate with low resistance coefficient and good impact toughness. The P/M slide plate materials can form lubricating film which results in a low friction coefficient. The replacement of the pure carbon slide plate by the P/M slide plate reduces the wear of contact wire and improves the service life of the slide plate. In the early 1980s, the P/M slide plate has become a typical product for the railway pantograph material in China.

However, P/M slide plate has certain limitations. Due to the low oil content, when the formed lubricating film is damaged or failed, it is difficult for the P/M slide plate to form a novel lubricating film to maintain the smooth contact between the pantograph slide and the contact wire, resulting in a serious wear of the pantograph slide on the contact wire [74–76]. In order to reduce the wear of contact wire and improve the service life of slide plate, the wear-resistant and wear-reducing components and solid lubricant were added into P/M slide plate [77–79]. In addition, improving the assembly method of the slide plate, such as adding carbon slider on the inner side of the P/M slide plate was used to improve the lubricity of the material. A mechanical composite copper matrix P/M slide plate was developed in China in the 1990s. The solid lubricant was added to the copper matrix P/M slide plate, which greatly reduced the wear of contact wire and provided lubrication during service. Although the P/M slide plate has been improved, it still cannot meet the requirements of the rapid development of high-speed railways for the performance of pantograph slide, and its application is partially restricted [80].

3.2.3 Metal impregnated carbon slide plate

3.2.3.1 Development history In the 1980s, the metal impregnated carbon slide plate materials with low resistivity and high mechanical strength were developed in Japan, and gradually replaced the P/M slide plate [81–83]. The electrified railway in Britain began to use the metal impregnated carbon slide plate in 1987. The metal impregnated carbon slide plate developed in Britain has lower resistivity and wear rate than the traditional pantograph slide materials and was widely used in European countries.

In the late 1980s, China's Academy of Railway Sciences, Zhengzhou Railway Bureau, and some other institutes successfully developed the metal impregnated carbon slide plate named 'SAC type aluminum coated metal impregnated carbon slide plate', which is suitable not only for the copper wire, but also for the mixed section of copper and steel aluminum wire. In 1991, a new type of SK_2 metal impregnated carbon slide plate was developed in China, which make up for the shortcomings and defects of the pure carbon slide and P/M slide plate. In recent years, the fabrication technology of pantograph slide in China has developed rapidly. The developed metal impregnated carbon slide plate has already realized large-scale production, and has been widely applied to freight railways by Beijing Railway Bureau to replace the imported metal impregnated carbon slide plate [70].

3.2.3.2 Fabrication technology The metal impregnated carbon slide plate material mainly consists of copper and

Table 5 The composition of copper matrix slide plate by mass (%) [74–77, 79]

Cu	Fe	Ni	Ti	Lubrication components		
				Pb	C	Else
70–80	5–10	1–5	3–8	0–3	1–3	1–2

copper alloy impregnated with pure carbon matrix. The porous carbon blank is prepared through a process which is similar to that of the pure carbon slide plate. After that, the copper or copper alloy is impregnated into the carbon blank by pressure impregnation. Thereby, a metal impregnated carbon material is obtained, and the mixed copper or copper alloy shows a network distribution in the carbon blank. The production process of the metal impregnated carbon slide plate is shown in Fig. 19 (red line). The metal is formed with a skeleton structure, which plays a role of reinforcement, as well as reducing the resistivity and porosity [84].

The interfacial bonding strength of metal and carbon matrix determines the comprehensive performance of the metal impregnated carbon slide materials, as the wettability is the key to the interfacial bonding strength of the material [85–87]. The main preparation method of metal impregnated slide plate is based on melt infiltration method which can be achieved in a container with high pressure, atmospheric pressure, and negative pressure at high temperature. It can be divided into pressure impregnation [88–90], pressureless melt infiltration [91, 92], and negative pressure infiltration [93, 94].

As mentioned above, the pressure impregnation method was initially used for the preparation of the metal impregnated carbon slide plate. The platform of pressure impregnation is shown in Fig. 20. The high density of the prepared composite and high utilization of copper alloy can be achieved by pressure impregnation. However, the obtained wettability of copper and carbon is very poor. Therefore, if the vacuum pressure impregnation is not used, it is difficult to impregnate the copper melt into the carbon matrix. Even if the impregnation is successful, the performance of the prepared pantograph slider would not be stable. In addition, the preparation of slide plate materials using the pressure impregnation method is very complex with low operational safety. These drawbacks prevented the industrialization application of this technique, and to develop pantograph slide materials with simple process and stable performance is required.

An improved technique has been developed by using the pressure impregnation method to make the alloy melt easily to impregnate or even impregnate the carbon matrix under ambient pressure [95]. Zuo et al. [96] proposed a strategy based on copper–boron alloying to improve the C/Cu interfacial bonding force, and the Cu–B/sintered-carbon composites were successfully prepared by pressure impregnation. The results showed that the C/Cu contact angle decreased from 123.6° to 21.3° in the case of 2.5% (by mass) B doping (see Fig. 21), and the compressive and flexural strengths of the modified composites were increased by 39% and 54%, respectively. Rambo et al. [97] used the pressureless melt infiltration method to form dense C/Cu composites by infiltrating Cu–Ti alloy into carbon preforms prepared by 3D printing under an argon gas protected pressureless condition. Negative pressure infiltration, on the other hand, is a way in which infiltration occurs under vacuum. To infiltrate the molten metal into the porous body, Yang et al. [98] prepared C/C–Cu composites with density of 2.7–4.9 g/cm^3 by placing Cu–Ti alloy melt infiltrated and C/C blanks in a sealed container at 1300 °C under 10^{-2} Pa.

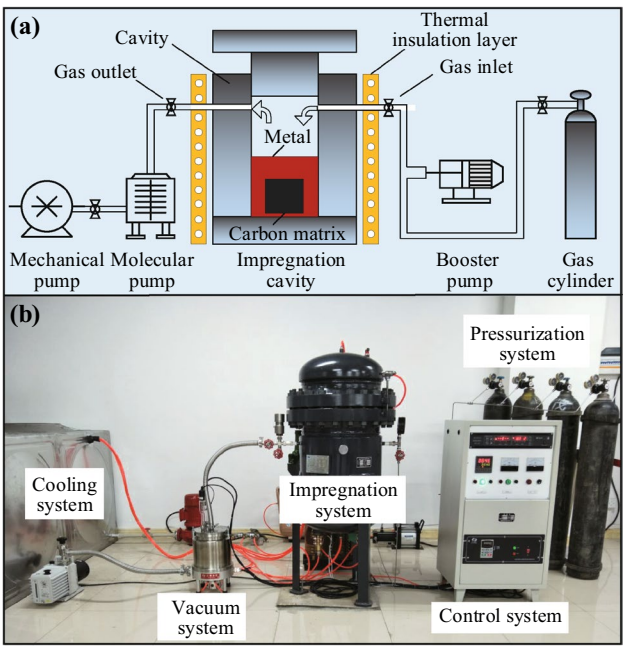

Fig. 20 Pressure impregnation experimental platform: **a** overall design scheme of experimental equipment; **b** experimental equipment

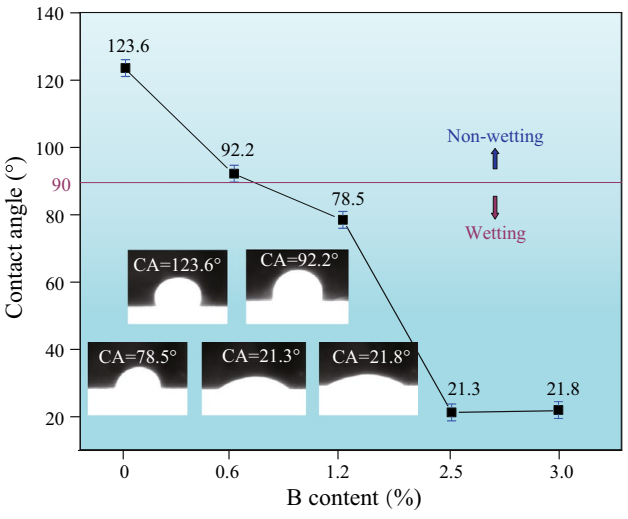

Fig. 21 Variation of contact angle with B content. As the mass fraction of B increase to 2.5%, the C/Cu contact angle decreases from 123.6 to 21.3 (modified after [96])

This method has low cost and is easy to be applied industrially. In addition, the prepared composites have better interfacial bonding and excellent overall performance, and the preparation of C/Cu composites by negative pressure infiltration technology has been widely used at present.

In recent years, in addition to the use of copper alloy impregnated carbon matrix, pure aluminum or aluminum alloy have been found to have potential advantages in preparing high electrical conductivity and light weight metal impregnated carbon slide plate. For example, aluminum/sintered carbon composites with good mechanical properties were prepared by using aluminum alloy to infiltrate the sintered carbon matrix under high pressure [99].

Table 6 shows a comparison of mechanical properties for the metal impregnated carbon slide plates developed in different countries. The hardness, electrical conductivity, flexural strength, and impact strength of the metal impregnated carbon slide plate produced in China have reached or even exceeded those of Germany, Britain and other advanced countries.

3.2.3.3 Advantages and limitations The metal impregnated carbon slide plate has many advantages compared to the P/M slide plate, as it is more suitable for the pantograph of high-speed electric locomotive [100]. It not only retains the advantages of pure carbon slide plate, such as good lubricity and wear resistance, but also solves the problem of the fast wear of the contact wire and improve the safety and reliability of the pantograph in the sliding of the contact wire [101–103]. It has been verified that the loss of metal impregnated carbon slide plate on copper wire is only 1/6–1/4 of that of P/M slide plate. Its own wear amount is 2.2 times of that of P/M slide plate and 1/4–1/3 of that of pure carbon slide plate [104]. As an ideal pantograph slide in copper wire section, the metal impregnated carbon slide plate plays a leading role in the field of electric locomotive pantograph in China in recent years.

However, the metal impregnated carbon slide plate has drawbacks such as complex preparation process, and high production and maintenance costs. In addition, with the continuous acceleration of high-speed railways, this type of slide plates often crack and partially fall. The weak interfacial bonding between carbon and copper leads to poor mechanical properties of metal impregnated carbon slide plates, which limits their application to railways at higher speed levels in the future.

3.2.4 Composite slide plate

3.2.4.1 Fiber reinforced composite slide plate The fiber reinforced composite slide plate is developed to reduce resistivity, improve impact toughness and wear resistance [105]. The fiber reinforced composite slide plates, which combines the advantage of the excellent self-lubrication of pure carbon slide plate and excellent mechanical properties, are mainly divided into two categories: carbon/metal fiber composite slide plates and carbon/carbon composite (C/Cs) slide plates.

Carbon/metal fiber composite slide plates are made of composite materials obtained by reinforcing the carbon matrix with metal fibers, metal powder, wire mesh or their mixtures, using an appropriate mixing method to make the reinforcement uniformly distributed in the matrix. The mixtures are pressed at a certain temperature and sintered at high temperature. The production process is shown in Fig. 19 (orange line). In order to improve the overall strength of carbon composite materials, chemical treatments need to be performed on the fibers to inhibit the carbonization trend of the metal fibers. Deng et al. [106] prepared carbon fiber/copper mesh knitted fabric reinforced carbon (CF/Cu/C) composites by chemical vapor infiltration. This kind of pantograph slide plates takes into account the high electrical conductivity of a pure carbon slide plate together with the high mechanical properties and good thermal conductivity of a metal slide plate. The density of this composite was tested to be 2.08 g/cm^3, the bending strength was 264.07 MPa, the compression strength was 288.13 MPa, and the electrical resistivity was 1.67 μΩ·m. However, once the reinforcing phase of carbon/metal fiber slide plate is damaged, the electrical conductivity will deteriorate seriously. In addition, due to the wide distribution of metal fibers in the carbon matrix, the wear of the contact wire is more serious.

The formation of C/Cs slide plate can be divided into two cases. In the first case, the blanks for formation of C/Cs slide

Table 6 Some key parameters of metal impregnated carbon slide plates in different countries [73, 81, 86–88]

Country	Density (g·cm^{-3})	Hardness (HS)	Electrical conductivity (×10^5 S·m^{-1})	Flexural strength (MPa)	Impact strength (J·cm^{-2})
Germany	2.25	100	2.30	80	0.23
Britain	2.41	95	4.48	84	0.22
France	2.30	75	3.71	60	0.26
Japan	2.60	100	1.11	85	0.31
China	2.50	118	5.41	85	0.35

plate are made of continuous CF. The carbon matrix is introduced into the blanks for densification and reinforcement by either chemical vapor deposition or resin/pitch impregnation carbonization to obtain C/Cs blanks. After that, the blanks are impregnated several times to obtain the C/Cs slide plate [107–110]. In the work performed by Yuan et al. [111], the CF reinforced pantograph slide was prepared by hot pressing technology using the modified phenolic resin and the continuous CF as the binder and the reinforced phase, respectively. The copper and the graphite were also used as conductive and lubricating phases, respectively. The results showed that with low resistivity, good impact resistance, good flexural strength and high compressive resistance, this pantograph slide can meet the performance requirements of the national standard for the pantograph slide widely used.

In the second case, short-cut CFs, continuous long CFs, and copper-plated CFs are usually used as reinforcements to improve the performance of the existing slide plate and enhance the overall performance of the composite materials [112, 113]. In the early twenty-first century, China developed a new type of pantograph slide using CF reinforced carbon matrix composite materials. The slide plate was made of copper-plated graphite powder and copper-plated coke powder, short carbon fibers were used as the reinforcing phase and the thermosetting resin as the binder. The raw materials were mixed sufficiently and then cold pressed or hot pressed to complete the process. The material not only has excellent friction and wear properties, but also has good mechanical and conductive properties. However, its long production cycle and high cost make it difficult to be applied in real applications. Yang and Dong [114] studied the mechanical properties and wear behavior of short carbon fiber reinforced copper matrix composites. Composites containing different amounts of carbon fibers were prepared by hot pressing technique. It was found that the carbon fiber/CuNiFe composites have higher performance in hardness, wear resistance and bending strength than the common copper alloy when carbon fibers content is less than 15% by volume.

However, because the preparation process of CF includes carbonization or graphitization, the stacking orientation of carbon atoms on the surface of CF is more consistent, and the atomic layer spacing is smaller. As a result, the surface of CF is chemically inert; the CF surface has the disadvantages of hydrophobicity, smoothness, and low adsorption property, which lead to poor interfacial bonding between CF and matrix. Therefore, it is necessary to modify the surface of CF to improve its interfacial bonding strength with the matrix. To solve this problem, three modification methods are proposed (see Fig. 22): (1) To improve the surface activity and surface free energy by introducing functional groups or molecular chains. (2) To increase the contact area with the resin infiltration, and form a mechanical interlock between the CF and the matrix by increasing the surface

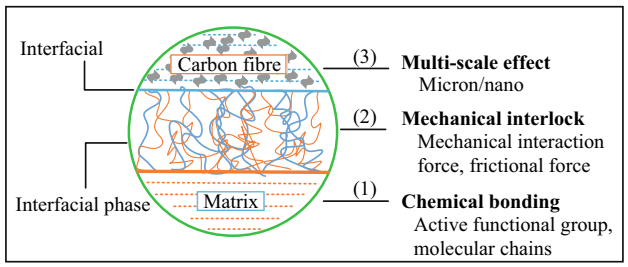

Fig. 22 Three modification methods to reinforce the interfacial bonding between carbon fiber and matrix

roughness and the specific surface area. (3) To improve the adhesion of the CF/resin interface by adsorbing or growing micro–nanoparticles on the surface of CF to reconstruct the surface. By this approach, a new three-dimensional structure of the CF surface can be obtained without bringing damage to the CF body.

Due to the special surface structure of CF, different surface treatment methods have been proposed for CF [115–119], which include liquid phase oxidation [120–122], plasma modification [123–125], electrochemical anodization [126–128] and surface multi-scale modification [129, 130]. In Ref. [131], a thin pyrocarbon (PyC) interface layer was deposited on the surface of CF to optimize the fiber/matrix (F/M) interfacial bonding, and then carbon nanotubes (CNTs) with radial orientation were grown on the CF surface by double injection chemical vapor deposition (DICVD) to modify the microstructure of the matrix (see Fig. 23). By this design, the flexural strength of C/Cs, the flexural ductility, the compressive strength, and the interlaminar shear strength have been significantly increased by 31.5%, 118%, 81.5%, and 82%, respectively. In Ref. [132], Poly (oxypropylene) Diamine (D_{400}) was used as a bridging agent to graft size-controlled graphene oxide flakes onto CF to improve the interfacial properties of CF composites. The results showed that the interfacial shear strength (IFSS) of middle sized graphene oxide sheets grafted CF/epoxy composites reached 82.2 MPa, with an enhancement of 75.6% compared with the untreated CF. The strong mechanical interlocking between CF and epoxy resin, as well as the improved wettability of resin on CF surface, were responsible for the enhancement of IFSS.

Li et al. [133] used pre-oxidized CF as the reinforcing phase of CF–C/Cs composites. Due to the abundant oxygen-containing functional groups on the surface of the pre-oxidized CF and the adaptive expansion when carbonized with pitch, the pre-oxidized CF reinforced C/Cs obtains an excellent fiber/matrix interfacial structure. The interfacial bonding mechanism and cross-sectional SEM images of CF–C/Cs and OPF–C/Cs are shown in Fig. 24a and Fig. 24e and f. The

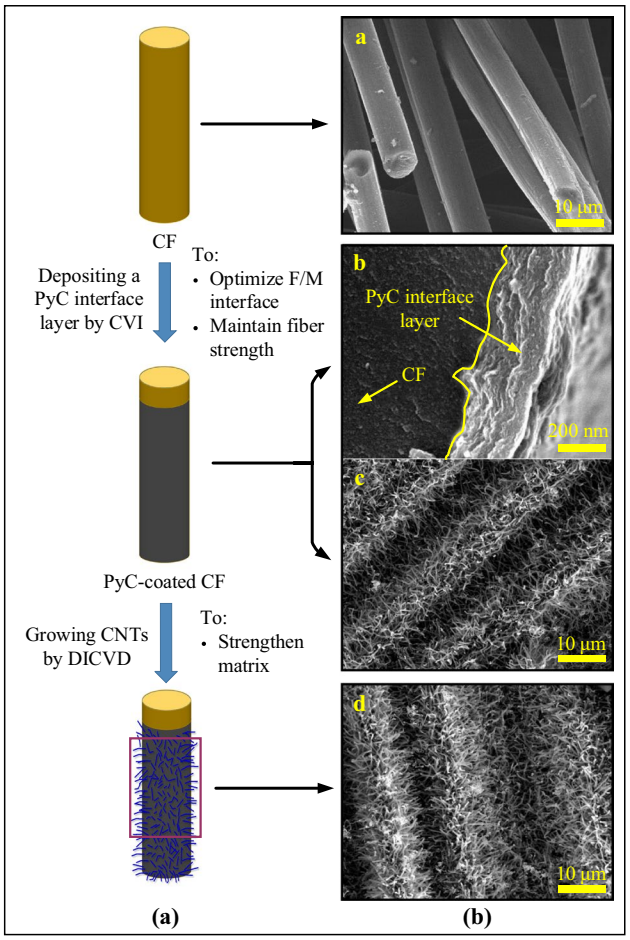

Fig. 23 **a** Schematic of depositing PyC interface layer on CF followed by growth of radial CNTs by DICVD and **b** SEM images corresponding to each stage [131]

compressive stress–strain curves of the three composites are shown in Fig. 24b. As shown in Fig. 24c and d, compared with the CF reinforced C/Cs, the flexural strength and impact strength of the pre-oxidized CF reinforced C/Cs increased by 31.8% and 53.3%, respectively. Due to the better interfacial bonding, the fracture mode was changed from plastic fracture to pseudoplastic fracture, which was beneficial to improving the ductility and toughness of the pantograph slide.

The above-mentioned studies have improved properties such as flexural strength and impact strength of the composite slide plates. However, comprehensive performance still needs to be improved. Therefore, the research direction of the novel composite materials in the slide plate should be focused on the improvement of the comprehensive performance to meet the requirements of pantograph slides of ultra-high-speed trains in the future.

3.2.4.2 Multi-carbide composite slide plate Multi-carbide composite (MCC) slide plate is made of multi-carbide matrix composite materials based on ternary-layered MAX phase ceramics (MAX phase: $M_{n+1}AX_n$, where M is a transition metal atom, A is a IIIA or IVA group atom, X is a C or N, and $n = 1, 2, 3\ldots$). The MAX phase ceramics are represented by Ti_3SiC_2 and Ti_3AlC_2. Its electrical conductivity is one order of magnitude higher than that of graphite, and its mechanical properties such as strength, toughness, and hardness are much better than that of graphite. Moreover, the friction coefficient of the MAX phase ceramics is lower, and the MAX phase ceramics have a good oxidation resistance at 1300°C which is much higher than that of graphite. Ti_3SiC_2 is a ternary layered compound, and due to its spatial structure, it has the excellent performance of both metals and ceramics in electrical conductivity, thermal conductivity, machinability, and self-lubrication [134–137]. Jiang et al. [138] found that adding Ti_3SiC_2 to C/Cu composite can improve its strength, hardness, and wear resistance without affecting its self-lubrication and electrical conductivity.

The addition of MAX phase ceramics to pantograph slide has become a research focus in recent years. Doping Ti_3SiC_2 in the matrix plays a significant role in lubrication and dispersion strengthening, as the prepared MCC slide plate material has better mechanical performances [139, 140]. The MCC slide plates are characterized by good electrical conductivity, high impact resistance, high wear resistance, high arc ablation resistance, and low wear on the contact wire, which will effectively solve the problems of fast wear, easy breakage, and large damage occurring to the contact wires of carbon matrix slide plates.

However, due to the nature of ceramic material retained by MCC slide plate, its stability needs to be improved. In addition, the material density is higher than that of carbon slide plate, which increases the load loss of pantograph. Due to the limitation of purity in the preparation process of Ti_3SiC_2 powder, it is still in the experimental stage and has not been produced on a large scale. Therefore, after further improvement of its stability, the MCC slide plate has a high possibility to be used as an ideal choice for the pantograph slide of ultra-high speed train in the future.

To sum up, with the increase of the train operation speed, the materials of pantograph slide have mainly experienced the process of metal, carbon, powder metallurgy, metal impregnated carbon and composite. The application field, advantage and disadvantage of different types of pantograph slide plates are shown in Table 7.

4 Detection and evaluation of pantograph–catenary system

In the electrified railway system, due to the long-term contact between pantograph slide and contact wire, the surface

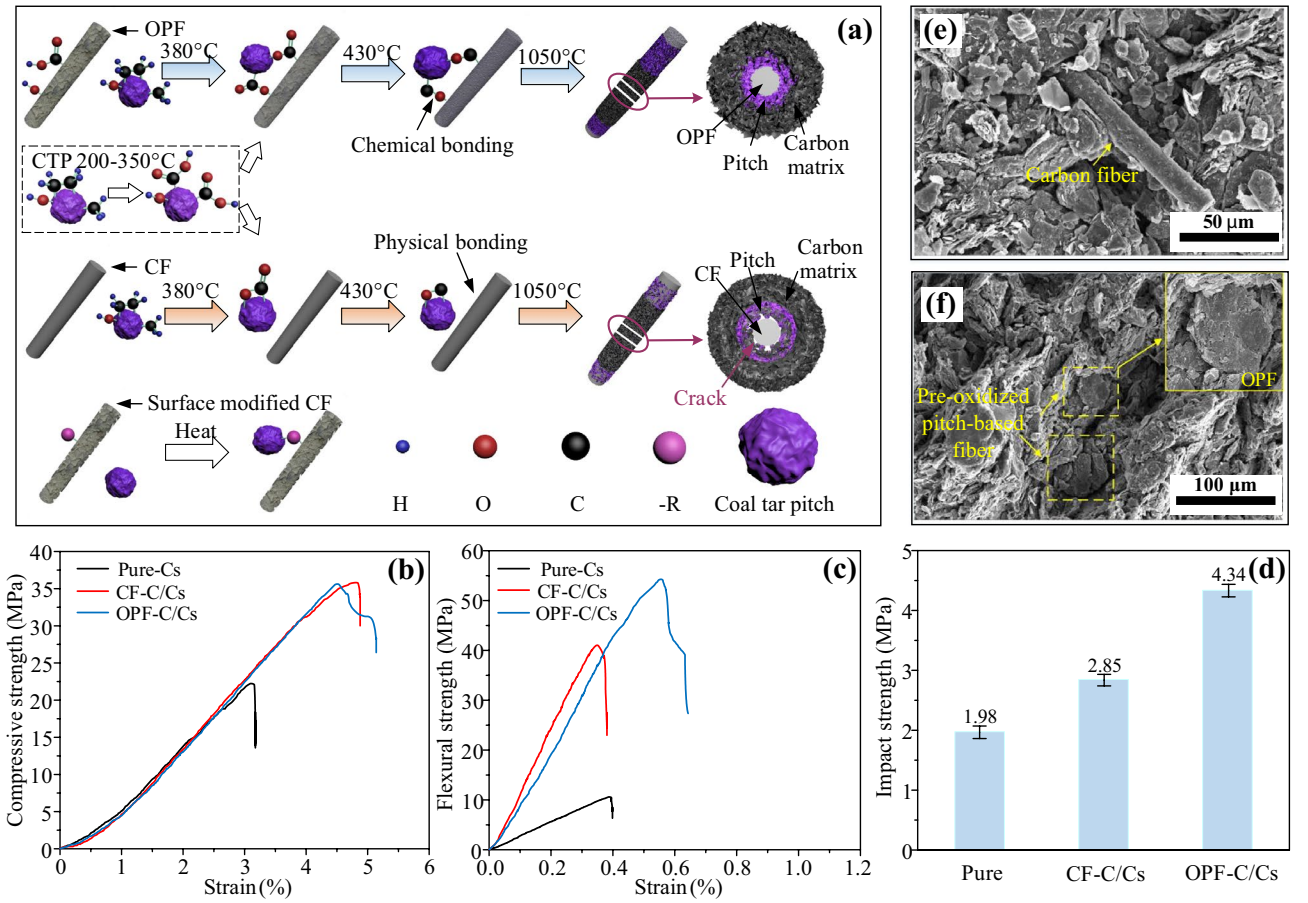

Fig. 24 **a** Interfacial bonding mechanism of C/Cs and OPF–C/Cs; **b–d** mechanical properties of pure-C/Cs, CF–C/Cs, and OPF–C/Cs (**b** compressive strength, **c** flexural strength, and **d** impact strength); **e** cross-sectional SEM images of CF–C/Cs; and **f** OPF–C/Cs [133]

of electrical contact material is worn under the joint action of sliding wear, arc erosion and temperature stress, gradually leading to internal cracks. This causes irreversible damage to the slide plate.

If the defects cannot be detected in time, they could gradually expand and endanger the safety and stable running of the train [141–143]. The detection methods of the pantograph slide include manual detection, laser detection, ultrasonic detection, and image detection. Manual detection has been gradually replaced by other advanced detection methods. In the following content, we focus more on laser detection, ultrasonic detection, and image detection.

4.1 Laser detection

The detection system installed above the train emits a laser to the pantograph slide to realize the three-dimensional (3D) reconstruction figure of the slide plate. By this approach, the wear or crack of the slide plate can be obtained based on the processor online calculation. Its working principle and overall structure are shown in Fig. 25. The existing pantograph detection systems are developed based on the laser displacement sensor with anti-interference and accurate measurement capabilities [144, 145].

Dwarakanath et al. [146] developed a laser sensor-based non-contact pantograph slide online detection system. When the pantograph passes below the detection system, the laser transmitter emits three laser lines to the upper surface of the slide plate. The laser lines on the slide plate are photographed by the high-speed camera, and the 3D shape of the slide plate is reconstructed through the three-dimensional point cloud. On this basis, the wear of the slide plate can be detected.

The laser detection method can realize the 3D reconstruction of the pantograph slide, which is a future research direction. However, the laser sensor is expensive and easily influenced by illumination, which limits the further application of the laser method. Meanwhile, the 3D reconstruction is related to the structure shape of the pantograph, and it is difficult to realize the complete 3D reconstruction if the thickness of pantograph slide is small.

4.2 Ultrasonic detection

Ultrasonic detection is a non-destructive detection method using ultrasonic wave to detect the internal defects of the workpiece. The basic principle of the ultrasonic detection method is that the ultrasonic sensor installed above the pantograph slide sends ultrasonic waves to the slide plate, and the sound wave will be reflected when it meets the interface between two media with discontinuous medium or large acoustic impedance difference. The damage of the slide plate can be obtained according to the time between ultrasonic emission and reception combined with the propagation speed of ultrasonic in the air [147–149]. Its working principle and overall structure are shown in Fig. 26.

For the detection of pantograph slide surface wear, Aydin [150] proposed a novel type of the pantograph slide fault detection method to automatically locate the pantograph fault area, which can effectively eliminate the influence of weather and other factors on image quality. Ostlund et al. [151] proposed an online automatic detection method of pantograph by using pattern recognition technology. The system analyzes the collected pantograph image and uses template matching to obtain the wear value of the pantograph slide.

Based on the Rayleigh integral theory, Wei et al. [152] established a Rayleigh integral model of ultrasonic propagation in pantograph slide. The optimum range of the probe parameters was determined by studying the distribution law of the ultrasonic field inside the pantograph slide under different probe frequencies and diameters. The differences of probe parameters between single and multiple cracks were compared. This method provides a theoretical basis for the evaluation of the internal damage degree of pantograph slide. The ultrasonic field distribution using different ultrasonic frequencies and different probe diameters are shown in Fig. 27.

The ultrasonic detection method [153] has the advantages of convenience, low cost, high detection efficiency, and high precision. But this method could be affected by environmental factors such as temperature, humidity, wind speed, and ambient noise.

4.3 Image detection

The image detection method mainly uses two sets of CCD (charge coupled device) cameras to capture pantograph images, and uses image processing technology to perform image filtering, image enhancement, edge detection, and information extraction on pantograph images. Its detection principle and overall structure are shown in Fig. 28. The use of image processing technology can improve the image quality, and has advantages in many aspects such as detection

Table 7 The application field, advantage and disadvantage of different types of pantograph slide plates

Types	Advantage	Disadvantage	Application field
Pure metal slide plate	High mechanical strength, excellent electrical conductivity, low cost, long service life	Poor lubrication, severe damage to the contact wire	Used in the early low-speed railway, but no longer used now
Pure carbon slide plate	Excellent self-lubricity, good anti-friction property, small damage of contact wire	Low flexural strength, poor impact strength, short service life, low electrical conductivity	Used in metro, urban rail transit, low-speed and medium-speed railway
Powder metallurgy slide plate	Excellent flexural strength, high impact strength, high electrical conductivity, not easy break, no uneven wear	Loose structure, low oil content, lubricating film easy failed, damage to the contact wire	Mainly used in heavy-duty freight railway
Metal impregnated carbon slide plate	Good flexural strength, good lubricity and wear resistance, good electrical conductivity	Complex preparation process, high cost, easy to crack and partially fall	Widely used in metro, urban rail transit, low-speed and high-speed railway
Composite slide plate	High electrical conductivity, high mechanical strength, low density, good lubricity and wear resistance		Development stage, to be used for ultra-high-speed railway

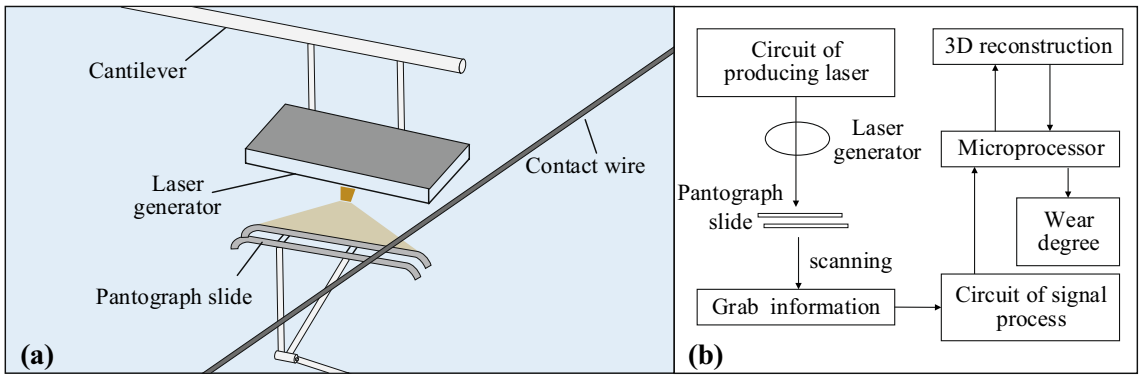

Fig. 25 Schematic diagram of laser detection: **a** overall structure and equipment installation; **b** working principle

accuracy, detection efficiency and adaptation to train speed [154, 155].

The key of image detection method is image processing. In [156], region-based-convolutional neural network (R-CNN) was used to extract the ROI (Regions of Interest) of the slide plate, as the wear size of the slide plate was detected based on the least square method and laser line. Aydin et al. [157] provide a method based on image processing and pattern recognition for online monitoring of the pantograph–catenary system. The images and data are provided to a D-Markov based state machine, so that faults such as overheating and pantograph arc can be identified. In [158], Gaussian homomorphic filtering and a variety of edge extraction algorithms were used to detect the wear of pantograph slide, and wavelet operator was used to detect the edge of pantograph slide more effectively. Although different image processing methods proposed in the above studies produced promising detection results, they all are in the experimental development stage.

In addition, some researchers [159–161] introduced a Pancam locomotive pantograph online monitoring system to detect the condition of the slide plate and the state of the ram's horn, and extracted the image target using the designed image target extraction algorithm. However, the system required the train to return to the depot to collect pantograph images in static conditions and its image processing method was more complex. Hu et al. [162] located the slide plate based on the line projection transformation principle, and used the adaptive Canny edge detection algorithm and the sub-pixel edge detection algorithm based on cubic polynomial fitting to realize the wear detection of pantograph slide.

In addition to the surface wear detection of pantograph slide, the image detection technology can also realize crack detection. The curve coefficient directional mapping algorithm and the second-generation curve detection algorithm based on moving parallel windows can effectively distinguish the line singularity features of slide crack images from the point singularity features of other interference images, and accurately detect and locate the crack damage of slide plate with an accuracy rate of 94.1% [163–166].

The pantograph image detection technology is now developing rapidly, but it still cannot realize comprehensive online detection. More efforts should be made on new algorithms. Apart from that, the study of image acquisition equipment with higher resolution, efficiency, and precision is still needed.

4.4 Evaluation of pantograph slide

The pantograph–catenary electrical contact system is designed to cater to trains running conditions, i.e., high-speed sliding, high current transmission, and complex operational environment for a long time. Once the pantograph–catenary system fails, the current collection quality of the train will be affected, which may cause the train to stop running and has a significant impact on the safety of passengers and transportation. Therefore, in addition to the damage detection of pantograph slide, it is also important to evaluate the current collection condition of pantograph slide. The high voltage team of Southwest Jiaotong University developed an electrical contact current collection condition detection system based on the acoustic-photic-electric multi-information fusion [167], which is a comprehensive evaluation system covering 'characteristic parameters-detection technology-condition evaluation' (see Fig. 29). The system can effectively evaluate the service performance of the pantograph–catenary electrical contact current collection system of high-speed train.

At present, there are still some deficiencies in the existing evaluation methods of pantograph slide. Accurate in-situ

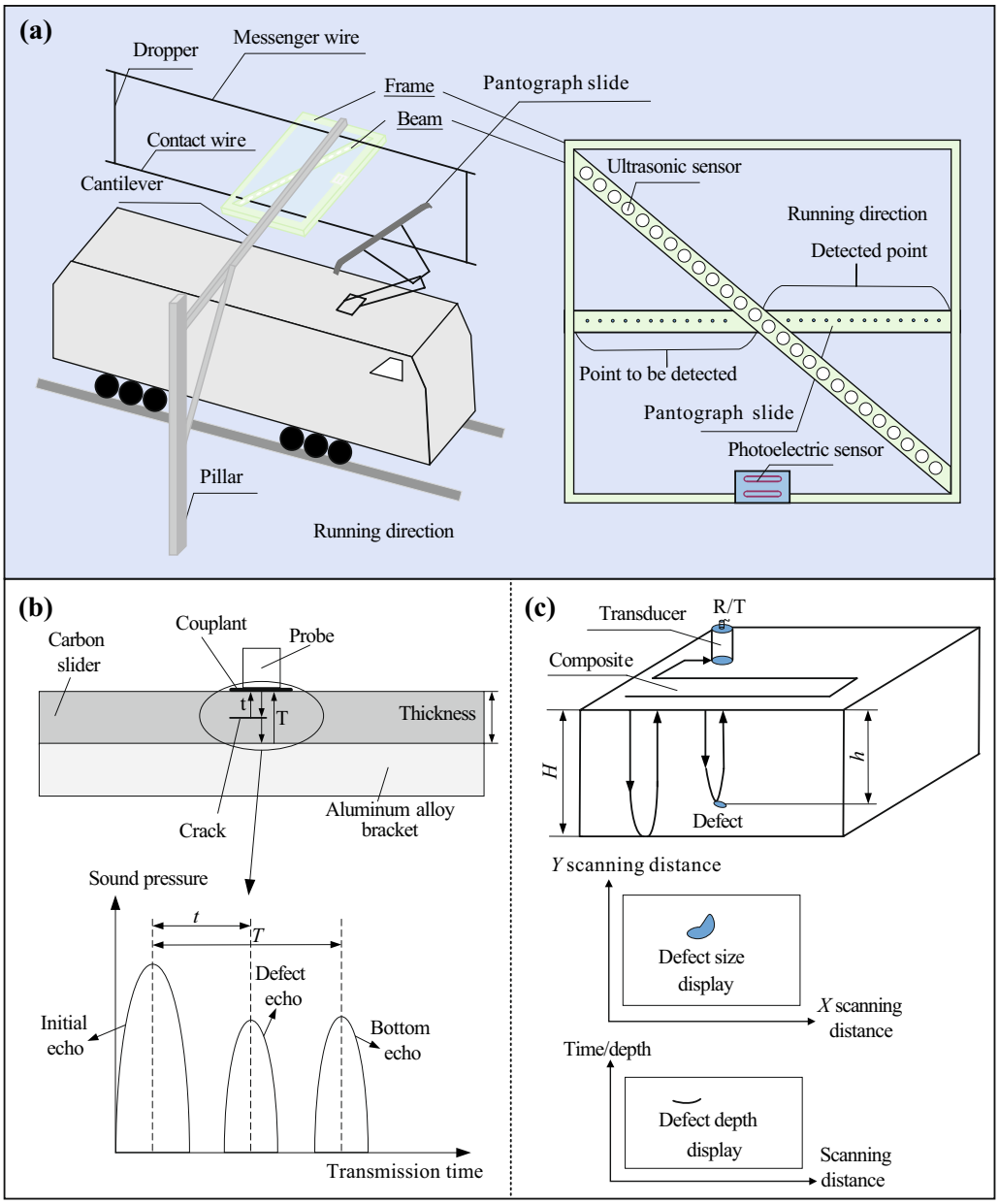

Fig. 26 Schematic diagram of ultrasonic detection: **a** overall structure and equipment installation; **b** working principle of surface wear; **c** working principle of inner damage

detection and online early warning cannot be achieved. What's more, it is still unknown if the detection accuracy of these methods could hold for ultra-high-speed trains in the future.

5 Challenges and outlooks

5.1 Challenges

As the development of high-speed railways move toward higher speeds and more complex operational environments, the design of pantograph–catenary system will face more technique challenges. Since the traction power required increases exponentially with the running speed of the train, the pantograph–catenary electric contact system must meet the transmission capacity of extra high power. With the increase of the train operation speed, the difference between the train speed and the catenary fluctuation speed becomes larger; the deterioration of the pantograph–catenary matching condition will aggravate the mechanical, electrical, and material coupling damage. Meanwhile, high power makes the intensity of arc burning greater, leading to

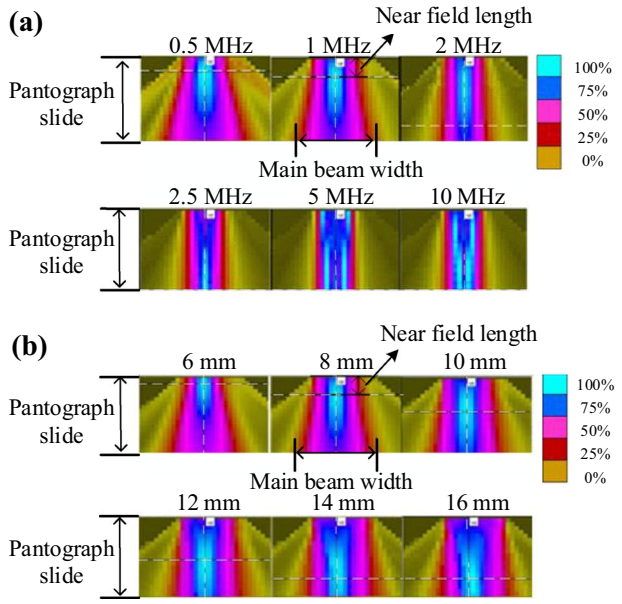

Fig. 27 Ultrasonic field distribution using **a** different ultrasonic frequencies and **b** different probe diameter

more serious ablation of the pantograph electrical contact system more serious. When the train is running, the pantograph–catenary electrical contact system is normally in a vibration state. Under high-speed conditions, the vibration and impact between pantograph and catenary will intensify, thus causing more serious cracking of the pantograph slide and even leading to the eccentric wear phenomenon of the pantograph slide. All these will seriously affect the service life of the pantograph–catenary electrical contact system. In addition, the current-carrying friction and wear of the pantograph–catenary electrical contact system are significantly affected by the current. When the train runs at a higher speed, the traction current increases greatly, and the wear of the pantograph slide and the contact wire becomes more serious, which will further shorten the service life of the pantograph–catenary contact system. Therefore, when the high-speed train runs at a higher speed in the future, higher requirements are placed on the pantograph–catenary electrical contact system.

The construction, operation and maintenance of high-speed railway pantograph–catenary system are facing severe challenges in the complex environments of various countries, such as the earthquakes in Japan, the floods in Germany and Britain, the heavy rainfalls in France, the heavy sandstorm, lightning, severe cold and high altitude environment in China. In earthquake and flood environment, it is necessary to conduct seismic design and flood-prevention design of catenary to prevent the collapse of catenary equipment caused by the earthquake and flood. In heavy rainfall and sandstorm environment, it is necessary to develop pantograph–catenary electrical contact materials with better comprehensive performance to reduce the severe wear of electrical contact materials caused by rainwater and sand grains. In thunder and lightning environments, the catenary needs to be designed with lightning protection to avoid serious damage to the pantograph–catenary system when the

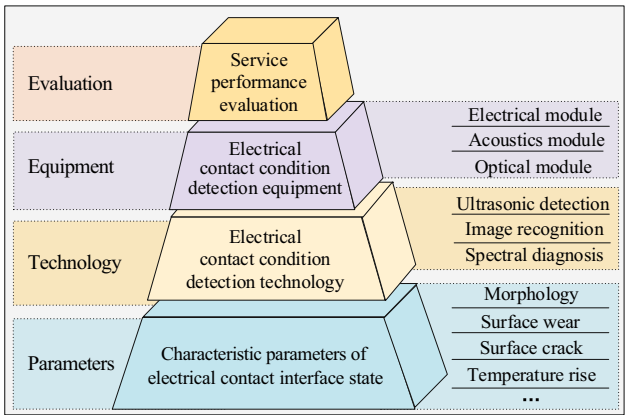

Fig. 29 Condition detection and evaluation system of the pantograph–catenary electrical contact system

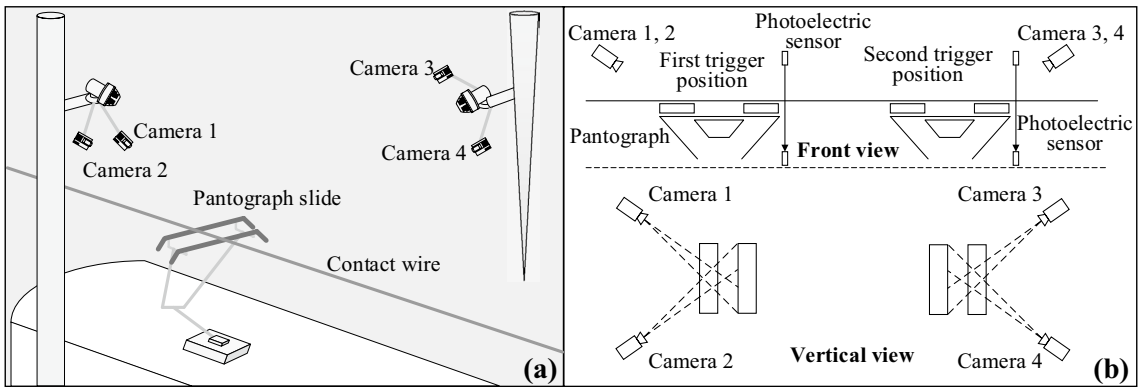

Fig. 28 Schematic diagram of image detection: **a** overall structure and equipment installation; **b** detection principle

high-speed train is struck by lightning. In the severe cold environment, it is necessary to conduct a deicing design for the pantograph–catenary system to reduce the damage of the pantograph–catenary system caused by frequent arcing occurrence.

At present, the Sichuan–Tibet Railway under construction in China is extremely difficult and is known as the most challenging railway project. The Sichuan–Tibet Railway has remarkable characteristics such as high altitude, crossing tunnel groups (over 80%), and a large number of unmanned areas; the line slope is as high as 30‰ (the highest in the world), the bridge span is large, and the operational environment is extremely harsh. As the most challenging railway project in human history, once a fault occurs and the power supply of the line is interrupted, rescue will be extremely difficult. Therefore, the Sichuan–Tibet Railway intends to use a rigid catenary power supply. For a high-speed rigid pantograph–catenary electrical contact system, there is no relevant design and operation experience all over the word. As the core equipment of energy transmission of high-speed train, the pantograph–catenary electrical contact system faces great technique challenges: Firstly, the rigid pantograph–catenary system has poor following performance, so the coupling vibration is severe during high-speed running, and the frequency of arcing occurrence increases significantly. Secondly, the low pressure caused by the high altitude significantly reduces the breakdown voltage of the air gap, resulting in a decrease in the threshold value of the train pantograph–catenary arc and its intensity. Thirdly, under the low pressure and strong airflow conditions, the maintenance time and extinguishing distance of the pantograph–catenary arc increase nonlinearly, and the distance between the support insulators of the Sichuan–Tibet railway catenary is small (the interval is about 6 m). These two factors cause the arcing to stretch and drift under the action of airflow, which is easy to develop rapidly on the catenary busbar, and even cause insulator string flash. Finally, the traction current transmission density is high when the train is climbing a long ramp, which leads to more serious corrosion of the electrical contact material by the pantograph arc. The above factors may accelerate the service performance degradation of the high-speed rigid pantograph–catenary system, reduce the current collection quality, and cause power supply interruption in severe cases. Therefore, the pantograph–catenary electrical contact system of the Sichuan–Tibet Railway need to overcome the above severe challenges from the extremely complex environments.

5.2 Outlooks

The improvement of the stability, reliability and service life of high-speed railway pantograph–catenary system is a key research direction in the future. To this end, the future work need to be conducted from the following aspects.

Firstly, for the catenary:

- Explore the type of catenary that is suitable for higher speed and increase the fluctuation speed of the catenary;
- Develop contact wire materials with better comprehensive performance using advanced large-scale heat treatment and processing equipment;
- Optimize production process, improve product reliability and reduce costs.

Secondly, for the pantograph:

- Explore the pantograph frame structure and pantograph head material with higher strength and lighter weight;
- Develop novel pantographs with better stability and following performance;
- Improve the matching performance between pantograph and catenary.

Thirdly, for the pantograph slide:

- Explore novel fabrication method for the metal impregnated carbon slide plate and improve its comprehensive mechanical properties;
- Explore advanced method to enhance the interfacial bonding strength between reinforcement and matrix;
- Develop brand-new composite slide plate with excellent comprehensive performance to improve the service life of pantograph slide.

Finally, for the detection:

- Develop high-precision online detection equipment for pantograph–catenary system;
- Improve the accuracy of online detection;
- Realize the in-situ detection and online early warning of the service condition of the pantograph–catenary system.

Last but not the least, increasing the loading capacity of high-speed railway is an important development direction in the future. At present, the high-speed train with the largest passenger capacity is China's CR400AF-S, with a passenger capacity of 1584. In 2020, China developed the world's first freight high-speed train with a speed of 350 km/h, with a cargo capacity nearly 110 t. Although the running of high-speed railway has reached a higher speed, its carrying capacity is small. For example, when a major disaster such as an earthquake or flood occurs in a country, a large number of disaster supplies and relief teams need to be sent to the disaster area at the first time. When a country is at war, it needs

to send a large number of heavy weapons and troops to the battlefield quickly. However, the carrying capacity of high-speed railways cannot meet these demands by far at present. Therefore, developing large loading capacity high-speed railways and improving their carrying capacity can not only promote the rapid development of the national economy, but also ensure the social stability and people's safety. The traction power of high-speed train with large carrying capacity is greatly improved, as its pantograph–catenary system must have greater current collection capacity and superior service performance.

Acknowledgements A great appreciation is given to Prof. Wanming Zhai for his invitation of this review article. The work was supported by the National Natural Science Foundation of China (Nos. U19A20105, 51837009, 51807167, 51922090, U1966602 and 52077182) and the Scientific and Technological Funds for Young Scientists of Sichuan (No. 2019JDJQ0019). The authors are grateful for the tremendous support provided by our project partners.

References

1. Yang HJ, Chen GX, Gao GQ, Wu GN, Zhang WH (2015) Experimental research on the friction and wear properties of a contact strip of a pantograph–catenary system at the sliding speed of 350 km/h with electric current. Wear 332–333:949–955
2. Wu G, Wei W, Gao G, Wu J, Zhou Y (2016) Evolution of the electrical contact of dynamic pantograph–catenary system. J Mod Transp 24(2):132–138
3. Uchide T, Imanishi K (2018) Underestimation of microearthquake size by the magnitude scale of the Japan meteorological agency: influence on earthquake statistics. JGR Solid Earth 123(1):606–620
4. Wada A (2016) Unusually rapid intensification of Typhoon Man-yi in 2013 under preexisting warm-water conditions near the Kuroshio front south of Japan. In: Nakamura H, Isobe A, Minobe S, Mitsudera H, Nonaka M, Suga T (eds) "Hot spots" in the climate system. Springer, Japan
5. Kenji S (2015) Geological and historical evidence of irregular recurrent earthquakes in Japan. Phil Trans R Soc A 373(2053):20140375
6. Blanchet J, Molinié G, Touati J (2018) Spatial analysis of trend in extreme daily rainfall in southern France. Clim Dyn 51(3):799–812
7. Fumière Q, Déqué M, Nuissier O, Somot S, Alias A, Caillaud C, Laurantin O, Seity Y (2020) Extreme rainfall in Mediterranean France during the fall: added value of the CNRM-AROME convection-permitting regional climate model. Clim Dyn 55(1–2):77–91
8. Luu LN, Vautard R, Yiou P, Van O (2018) Attribution of extreme rainfall events in the south of France using EURO-CORDEX simulations. Geophys Res Lett 45(12):6242–6250
9. Pöschmann JM, Kim D, Kronenberg R, Bernhofer C (2021) An analysis of temporal scaling behaviour of extreme rainfall in Germany based on radar precipitation QPE data. Nat Hazard Earth Sys 21(4):1195–1207
10. Tarasova L, Basso S, Poncelet C, Merz R (2018) Exploring controls on rainfall-runoff events: 2 regional patterns and spatial controls of event characteristics in Germany. Water Resour Res 54(10):7688–7710
11. Fekete A, Sandholz S (2021) Here comes the flood, but not failure? Lessons to learn after the heavy rain and pluvial floods in Germany. Water 13(21):3016
12. Ehmele F, Kunz M (2019) Flood-related extreme precipitation in southwestern Germany: development of a two-dimensional stochastic precipitation model. Hydrol Earth Syst Sci 23(2):1083–1102
13. Archer DR, Fowler HJ (2015) Characterising flash flood response to intense rainfall and impacts using historical information and gauged data in Britain. J Flood Risk Manag 11(S1):121–133
14. Wang H, Xuan Y (2021) Temporal and spatial variation of extreme rainfall in Great Britain and Australia using the SRS-GDA toolbox. In: 6th IAHR Europe Congress, Warsaw, Poland
15. Barnes AP, Svensson C, Kjeldsen TR (2021) North Atlantic air pressure and temperature conditions associated with heavy rainfall in Great Britain. Int J Climatol 42(5):3190–3207
16. Petrova EG (2011) Natural factors of technological accidents: the case of Russia. Nat Hazard Earth Sys 11(8):2227–2234
17. Golubev VN, Petrushina MN, Frolov DM (2016) Snowfalls on the territory of Russia in 1961–2015 and their ecological consequences. In: 9th International Geographical Union Conference Land use change, climate and disaster risk reduction. New Delhi, India
18. Cai Y, Li L, Ehsan E, Qiu Y (2018) Selection of policies on typhoon and rainstorm disasters in China: a content analysis perspective. Sustainability 10(2):387
19. He J, Wang X, Yu Z, Zeng R (2015) Statistical analysis on lightning performance of transmission lines in several regions of China. IEEE T Power Deliver 30(3):1543–1551
20. Zhao P, Zhou Y, Xiao H, Liu J, Gao J, Fei G (2017) Total lightning flash activity response to aerosol over China area. Atmosphere 8(2):26
21. Liu L, Lyu Y, Xu W, Wang J, Shi P (2016) Blown sand disasters in China. In: Natural Disasters in China. IHDP/Future Earth-Integrated Risk Governance Project Series. Springer, Berlin, Heidelberg
22. Friedrich K, Rainer P, Axel S (2001) Contact lines for electric railways. Publicis Corporate Publishing, Wrlangen, Germany
23. Moshe G (2006) Development and impact of the modern high-speed train: a review. Transp Rev 26(5):593–611
24. Antunes P, Mósca A, Ambrósio J, Pombo J, Pereira M (2012) Development of a computational tool for the dynamic analysis of the pantograph-catenary interaction for high-speed trains. In: proceedings of the eleventh international conference on computational structures technology, Dubrovnik, Croatia. Civil-Comp Press, Stirlingshire, UK
25. Vesali F, Rezvani M, Molatefi H, Hecht M (2018) Static form-finding of normal and defective catenaries based on the analytical exact solution of the tensile Euler-Bernoulli beam. Proc Inst Mech Eng Part F J Rail Rapid Transit 233(7):691–700
26. Nåvik P, Derosa S, Ronnquist A (2020) Development of an index for quantification of structural dynamic response in a railway catenary section. Eng Struct 222:111154

27. Park T, Kim B, Wang Y, Han C (2002) A catenary system analysis for studying the dynamic characteristics of a high speed rail pantograph. KSME Int J 16(4):436–447
28. He N, Liu JW, Wang L, Wang XY (2015) The study of wind resistance performance of electrified railway catenary in strong wind area. In: proceedings of the international conference on chemical, material and food engineering, advances in engineering research, vol 22, Kunming, Yunnan, China. Paris, France: Atlantis Press. pp 212–216
29. Wu J (2018) Pantograph and contact line system. Elsevier Publishing, Amsterdam, Holland
30. Park CB, Jeong G (2017) Thermal characteristics analysis of upper arm hybrid structure of lightweight pantograph considering heat source by collecting current. J Korean Soc Railw 20(4):466–473
31. Tan XM, Yang ZG, Tan XM, Wu XL, Zhang J (2018) Vortex structures and aeroacoustic performance of the flow field of the pantograph. J Sound Vib 432:17–32
32. Guan T, Liu X, Xuan L (2013) Raising torque calculation system design for single-arm pantograph. Adv Mat Res 655–657:603–607
33. Jia F, Xu F, Xia Z, Zhou H, Zhang D (2016) Fatigue properties of the pantograph–insulator system of metro trains: experiments and the design for improvement. J Mech Sci Technol 30(10):4549–4558
34. Jia F, Xu F, Zhou H et al (2017) Optimization and simulation of the operational motion of a pantograph: uplift and retraction. J Mech Sci Technol 31(1):41–52
35. Tanifuji K, Koizumi S, Shimamune R (2000) Mechatronics in Japanese rail vehicles: active and semi-active suspensions. IFAC Proc Vol 33(26):253–258
36. Hagiwara Y (2008) Environmentally-friendly aspects and innovative lightweight traction system technologies of the shinkansen high-speed EMUs. IEEJ T Electr Electr 3(2):176–182
37. Kobayasi T, Fujihasi Y, Tsuburaya T, Satoh J, Oura Y, Fujii Y (1998) Current collecting performance of overhead contact line–pantograph system at 425 km/h. Electr Eng Japan 124(3):73–81
38. Wang L, Gu H (2019) High-speed rail (HSR) and urban development. Studies on China's high-speed rail new town planning and development. Springer, Singapore, pp 1–19
39. Chater E, Ghani D, Giri F, Haloua M (2015) Output feedback control of pantograph–catenary system with adaptive estimation of catenary parameters. J Mod Transp 23(4):252–261
40. Kiessling F, Puschmann R, Schmieder A, Schneider E (2018) Contact lines for electric railways planning, design, implementation, maintenance. Railw Gaz Int 174(2):60–60
41. Song Y, Jiang T, Nåvik P et al (2021) Geometry deviation effects of railway catenaries on pantograph–catenary interaction: a case study in Norwegian railway system. Railw Eng Sci 29(4):350–361
42. Zhou L, Shen Z (2011) Progress in high-speed train technology around the world. J Mod Transp 19(1):1–6
43. Ruan J, Li A, Yan FW et al (2013) Dynamic performance simulation of overhead contact system for over 350km/h high-speed rail. Adv Mat Res 706–708(2):1305–1309
44. Liu P, Yang Y, Yao J, Wang W, Dong Z (2012) Experimental study on dynamic behaviors of concrete bridge in China existing railway speed increase to 200–250km/h. Appl Mech Mater 193–194:1123–1128
45. Liu Z, Song Y, Han Y, Wang H, Zhang J, Han Z (2018) Advances of research on high-speed railway catenary. J Mod Transp 26(1):1–23
46. Zhang W, Zhou N, Li R et al (2011) Pantograph and catenary system with double pantographs for high-speed trains at 350 km/h or higher. J Mod Transp 19(1):7–11
47. Edquist C, Hammarqvist P, Hommen L (2000) Public technology procurement in Sweden: the X2000 high speed train. In: Public Technology Procurement and Innovation, Springer, US
48. Zhen G, Kim Y, Li H (2014) Bending fatigue life evaluation of Cu-Mg alloy contact wire. Int J Precis Eng Man 15(7):1331–1335
49. Sakai Y, Inoue K, Asano T et al (1991) Development of high-strength, high-conductivity Cu-Ag alloys for high-field pulsed magnet use. Appl Phys Lett 59(23):2965–2967
50. Hu Y, Chen GX, Zhang SD et al (2017) Comparative investigation into the friction and wear behaviors of a Cu-Ag contact wire/carbon strip and a pure copper contact wire/carbon strip at high speeds. Wear 376–377:1552–1557
51. Bai Y, Liu W, Zhang J et al (2013) Study on influence of contact wire design parameters on contact characteristics of pantograph–catenary. In: IEEE international conference on intelligent rail transportation (ICIRT), Beijing, China, 2013. IEEE, p 269–273
52. Jia SG, Liu P, Ren FZ et al (2007) Sliding wear behavior of copper alloy contact wire against copper-based strip for high-speed electrified railways. Wear 262(7–8):772–777
53. Ma A, Zhu C, Chen J et al (2014) Grain refinement and high-performance of equal-channel angular pressed Cu–Mg alloy for electrical contact wire. Metals 4(4):586–596
54. Adachi K, Tsubokawa S, Takeuchi T et al (1997) Plastic deformation of Cr phase in Cu–Cr composite during cold rolling. J Jpn I Met 61(5):391–396
55. Hong SI, Kim PH, Choi YC (2004) High strain rate superplasticity of deformation processed Cu–Ag filamentary composites. Scr Mater 51(2):95–99
56. Jia SG, Liu P, Ren FZ et al (2005) Wear behavior of Cu–Ag–Cr alloy wire under electrical sliding. Mat Sci Eng A-Struct 398(1–2):262–267
57. Kim H, Hu Z, Thompson D (2020) Effect of cavity flow control on high-speed train pantograph and roof aerodynamic noise. Railw Eng Sci 28(1):54–74
58. Dai Z, Li T, Zhou N et al (2021) Numerical simulation and optimization of aerodynamic uplift force of a high-speed pantograph. Railw Eng Sci 30(1):117–128
59. Ambrósio J, Rauter F, Pombo J, Pereira M (2010) A flexible multibody pantograph model for the analysis of the catenary–pantograph contact. Multibody dynamics. Computational methods in applied sciences. Springer, Dordrecht, pp 1–27
60. Usuda T, Ikeda M, Yamashita Y (2011) Method for detecting step-shaped wear on contact strips by measuring catenary vibration. Q Rep RTRI 52(4):237–243
61. Bucca G, Collina A (2009) A procedure for the wear prediction of collector strip and contact wire in pantograph–catenary system. Wear 266(1–2):46–59
62. Liu XL, Li ZH, Hu MJ et al (2021) Research on the wear properties of carbon strips and contact wires at frigid temperatures. Wear 486–487:204112
63. Wu G, Zhou Y, Gao G, Wu J, Wei W (2018) Arc erosion characteristics of cu-impregnated carbon materials used for current collection in high-speed railways. IEEE Trans Compon Packag Manuf Technol 8(6):1–10
64. Bouchoucha S, Chekroud S, Paulmier D (2004) Influence of the electrical sliding speed on friction and wear processes in an electrical contact copper-stainless steel. Appl Surf Sci 223(4):330–342
65. Zuo H, Wei W, Yang Z et al (2021) Synchronously improved mechanical strength and electrical conductivity of carbon/copper composites by forming Fe3C interlayer at C/Cu interface. Mater Today Commun 28:102661
66. He DH, Manory RR, Grady N (1998) Wear of railway contact wires against current collector materials. Wear 215(1–2):146–155

67. Tsuchiya Z (1950) On the carbon slider of the pantograph current collector. TANSO 1(2):57–60
68. Ebeling K (2005) High-speed railways in Germany. Japan Railw Transp Rev 40:36–45
69. Xiong X, Tu C, Ding C, Zhang J, Chen J (2014) Arc erosion wear characteristics and mechanisms of pure carbon strip against copper under arcing conditions. Tribol Lett 53(1):293–301
70. Wu G, Gao G, Wei W et al (2019) Electric contact material of pantograph and catenary. The electrical contact of the pantograph-catenary system. Springer, Singapore, pp 195–220
71. Nagasawa H, Kato K (1998) Wear mechanism of copper alloy wire sliding against iron-base strip under electric current. Wear 216(2):179–183
72. Shang F, Zhou HX, Qiao B, Li H, Yi Q (2011) Application of metal powder metallurgy technology in preparation of friction materials of the railway vehicles. Adv Mater Res 287–290:2987–2990
73. Yoshitaka K (2016) Pantograph contact strip for Shinkansen and its lubrication technology. J Jpn Soc Tribologis 61(3):167–172
74. Wang H, Fang ZZ, Sun P (2010) A critical review of mechanical properties of powder metallurgy titanium. Int J Powder Metall 46(5):45–57
75. Lawley A, Murphy TF (2003) Metallography of powder metallurgy materials. Mater Charact 51(5):315–327
76. Masooth PHS, Bharathiraja G, Jayakumar V, Palani K (2022) Microstructure and mechanical characterisation of ZrO2 reinforced Ti6Al4V metal matrix composites by powder metallurgy method. Mater Res Express 9(2):020003
77. Pokorska I (2007) Modeling of powder metallurgy processes. Adv Powder Technol 18(5):503–539s
78. Yang L, Yao G, Lu Y (2005) Research on new and high performance electric locomotive pantograph slide plate. Mater Rev 19(11):136–139
79. Shangguan B, Zhang YZ, Xing JD et al (2012) Wear behavior of electrified copper–MoS2 powder metallurgy materials under dry sliding. J Comput Theor Nanos 9(9):1458–1461
80. Wang P, Wei F, Zhao Z, Guo Y, Hao Z (2021) Effect of heat treatment temperature on mechanical and tribological properties of copper impregnated carbon/carbon composite. Tribol Int 164:107209
81. Wei W, Li X, Yang Z, Huang Z, Zuo H, Wu G et al (2021) Highly conductive graphite matrix/copper composites by a pressureless infiltration method. J Appl Phys 130:015102
82. Wei Q, Xu LX, Shi HJ, Shao LF, Hao XZ (2011) Study on network structure C-Cu composites of pantograph slide plates. Adv Mater Res 150–151:941–946
83. He DH, Manory R (2001) A novel electrical contact material with improved self-lubrication for railway current collectors. Wear 249(7):626–636
84. Miroshkin NY, Gulevskii VA, Kidalov NA (2021) Carbon-graphite preparation for impregnation with aluminum alloy. IOP Conf Ser Mater Sci Eng 1129(1):012008
85. Zang J, Jing L, Wang Y, Zhang X, Yuan Y (2008) Study of the wettability between diamond abrasive and vitrified bond with low melting point and high strength. Key Eng Mater 359–360:11–14
86. Jarzbek DM (2018) The impact of weak interfacial bonding strength on mechanical properties of metal matrix-ceramic reinforced composites. Compos Struct 201:352–362
87. Liao Q, Wei W, Zuo H, Li X, Yang Z, Xiao S, Wu G (2020) Interfacial bonding enhancement and properties improvement of carbon/copper composites based on nickel doping. Compos Interfaces 28(6):637–649
88. Yang G, Jiang Y, Feng J et al (2017) Synthesis of fibre reinforced Al2O3-SiO2 aerogel composite with high density uniformity via a facile high-pressure impregnation approach. Process Appl Ceram 11(3):185–190
89. Li Y, Huang J, Wang M et al (2020) Microstructure and current carrying wear behaviors of copper/sintered-carbon composites for pantograph sliders. Met Mater Int 27(9):3398–3408
90. Cui L, Luo R, Cui G (2018) Effect of Al–Mg alloy infiltration on mechanical and electrical properties for carbon/carbon composites. Crystals 8(5):196
91. He BL, Zhu YF (2011) Microstructure and properties of TiC/Ni3Al composites prepared by pressureless melt infiltration with porous TiC/Ni3Al preforms. Mater Manuf Process 26(4):586–591
92. Cui L, Luo R, Wang L, Luo H, Deng C (2017) Novel copper-impregnated carbon strip for sliding contact materials. J Alloys Compd 735:1846–1853
93. Lu TJ, Chen F, He D (2000) Sound absorption of cellular metals with semiopen cells. J Acoust Soc Am 108(4):1697–1709
94. Braszczyńska-Malik KN, Kamieniak J (2017) AZ91 magnesium matrix foam composites with fly ash cenospheres fabricated by negative pressure infiltration technique. Mater Charact 128:209–216
95. Zuo H, Wei W, Li X et al (2022) Enhanced wetting and properties of carbon/copper composites by Cu-Fe alloying. Compos Interfaces 29(1):111–120
96. Zuo H, Wei W, Yang Z et al (2021) Performance enhancement of carbon/copper composites based on boron doping. J Alloys Compd 876:160213
97. Rambo CR, Travitzky N, Greil P (2014) Conductive TiC/Ti–Cu/C composites fabricated by Ti–Cu alloy reactive infiltration into 3D-printed carbon performs. J Compos Mater 49(16):1971–1976
98. Ran L, Peng K, Yi M, Yang L (2011) Ablation property of a C/C–Cu composite prepared by pressureless infiltration. Mater Lett 65(13):2076–2078
99. Ma S, Xu E, Zhu Z et al (2018) Mechanical and wear performances of aluminum/sintered-carbon composites produced by pressure infiltration for pantograph sliders. Powder Technol 326:54–61
100. Yin J, Zhang H, Tan C, Xiong X (2014) Effect of heat treatment temperature on sliding wear behaviour of C/C–Cu composites under electric current. Wear 312(1–2):91–95
101. Kong B, Ru J, Zhang H, Fan T (2018) Enhanced wetting and properties of carbon/carbon-Cu composites with Cr3C2 coatings by Cr-solution immersion method. J Mater Sci Technol 34(03):458–465
102. Shangguan B, Zhang Y, Xing J et al (2010) Comparative study on wear behaviors of metal- impregnated carbon material and C/C composite under electrical sliding. Tribol Trans 53(6):933–938
103. Smith RA (2004) Railway speed-up: a review of its history, technical developments and future prospects. JSME Int J, Ser C 47(2):444–450
104. Kubo S, Kato K (1999) Effect of arc discharge on the wear rate and wear mode transition of a copper-impregnated metallized carbon contact strip sliding against a copper disk. Tribol Int 32(7):367–378
105. Wang C, Yang X, Cai X et al (2016) Research on friction material with carbon fiber and melamine modified phenolic resin. Am J Mech Appl 4(1):20–24
106. Deng C, Zhang H, Yin J et al (2017) Carbon fiber/copper mesh reinforced carbon composite for sliding contact material. Mater Res Express 4(2):025602
107. Tu C, Chen Z, Xia J (2009) Thermal wear and electrical sliding wear behaviors of the polyimide modified polymer-matrix pantograph contact strip. Tribol Int 42(6):995–1003

108. Tu C, Hong L, Song T et al (2019) Superior mechanical properties of sulfonated graphene reinforced carbon-graphite composites. Carbon 148:378–386
109. Michaud V, Mortensen A (2001) Infiltration processing of fibre reinforced composites: governing phenomena. Compos Part A Appl Sci Manuf 32(8):981–996
110. Lin Y, Ran L, Yi M (2011) Carbon fiber knitted fabric reinforced copper composite for sliding contact material. Mater Des 32(4):2365–2369
111. Yuan H, Wang C, Lu W, Zhang S (2012) Preparation and tribological behavior of carbon fiber reinforced pantograph slide plate. Adv Mater Res 430–432:378–382
112. Xia L, Jia B, Zeng J, Xu J (2009) Wear and mechanical properties of carbon fiber reinforced copper alloy composites. Mater Charact 60(5):363–369
113. Liu L, Li W, Tang Y, Shen B, Hu W (2009) Friction and wear properties of short carbon fiber reinforced aluminum matrix composites. Wear 266(7–8):733–738
114. Yang L, Dong Y (2011) Wear and mechanical properties of short carbon fiber reinforced copper matrix composites. Key Eng Mater 474–476:1605–1610
115. Galanu U, Lin Y, Ehlert GJ et al (2011) Effect of Zn–ZnO nanowire morphology on the interfacial strength of nanowire coated carbon fibers. Compos Sci Technol 71(7):946–954
116. Kim KJ, Kim J, Yu WR et al (2013) Improved tensile strength of carbon fibers undergoing catalytic growth of carbon nanotubes on their surface. Carbon 54:258–267
117. Zhang T, Cheng Q, Xu Z, Jiang B, Huang Y (2019) Improved interfacial property of carbon fiber composites with carbon nanotube and graphene oxide as multi-scale synergetic reinforcements. Compos Part A: Appl Sci Manufac 125(13):105573
118. Han P, Ma L, Song G et al (2019) Strengthening and modulating interphases in carbon fiber/epoxy composites by grafting dendritic polyetheramine with different molecular weights onto carbon fiber. Polym Compos 40(S2):E1525–E1536
119. Sui K, Zhang Q, Liu Y, Lei T, Li L (2014) Improved interfacial and impact properties of carbon fiber/epoxy composites through grafting hyperbranched polyglycerols on a carbon fiber surface. e-Polymers 14(2):57–62
120. Xu Z, Wu X, Ying S et al (2008) Surface modification of carbon fiber by redox-induced graft polymerization of acrylic acid. J Appl Polym Sci 108:1887–1892
121. Zhao G, Wang T, Wang Q (2011) Surface modification of carbon fiber and its effects on the mechanical and tribological properties of the polyurethane composites. Polym Compos 32(11):1726–1733
122. Tiwari S, Bijwe J, Panier S (2011) Tribological studies on polyetherimide composites based on carbon fabric with optimized oxidation treatment. Wear 271(9–10):2252–2260
123. Xie J, Xin D, Cao H et al (2011) Improving carbon fiber adhesion to polyimide with atmospheric pressure plasma treatment. Surf Coat Technol 206(2–3):191–201
124. Tiwari S, Sharma M, Panier S et al (2011) Influence of cold remote nitrogen oxygen plasma treatment on carbon fabric and its composites with specialty polymers. J Mater Sci 46(4):964–974
125. Ma K, Wang B, Chen P, Zhou X (2011) Plasma treatment of carbon fibers: non-equilibrium dynamic adsorption and its effect on the mechanical properties of RTM fabricated composites. Appl Surf Sci 257(9):3824–3830
126. Fukunaga A, Ueda S, Nagumo M (1999) Air-oxidation and anodization of pitch-based carbon fibers. Carbon 37(7):1081–1085
127. Guo Y, Liu J, Liang J (2005) Surface state of carbon fibers modified by electrochemical oxidation. J Mater Sci Technol 21(3):371–375
128. Ma Y, Wang J, Cai X (2016) The effect of electrolyte on surface composite and microstructure of carbon fiber by electrochemical treatment. Int J Electrochem Sci 8(2):2806–2815
129. Yuan X, Zhu B, Cai X et al (2018) Micro-configuration controlled interfacial adhesion by grafting graphene oxide onto carbon fibers. Compos Part A Appl Sci Manuf 111:83–93
130. Monfaerd JS, Okan BS, Menceloglu YZ et al (2016) Nano-engineered design and manufacturing of high-performance epoxy matrix composites with carbon fiber/selectively integrated graphene as multi-scale reinforcements. RSC Adv 6(12):9495–9506
131. Feng L, Li K, Xue B, Fu Q, Zhang L (2017) Optimizing matrix and fiber/matrix interface to achieve combination of strength, ductility and toughness in carbon nanotube-reinforced carbon/carbon composites. Mater Des 113(5):9–16
132. Wang C, Li J, Yu J et al (2017) Grafting of size-controlled graphene oxide sheets onto carbon fiber for reinforcement of carbon fiber/epoxy composite interfacial strength. Compos Part A Appl Sci Manuf 101:511–520
133. Li X, Yang Z, Zhao Y et al (2022) Excellent interfacial structural integrity of pre-oxidized carbon fiber-reinforced carbon-carbon composites. Compos Interfaces 29(4):383–396
134. Zhang J, Liu W, Jin Y et al (2018) Study of the interfacial reaction between Ti3SiC2 particles and Al matrix. J Alloys Compd 738:1–9
135. Atazadeh N, Heydari MS, Baharvandi HR et al (2016) Reviewing the effects of different additives on the synthesis of the Ti3SiC2 MAX phase by mechanical alloying technique. Int J Refract Met H 61:67–78
136. Shang F, Sun W, Qiao B, He Y, Li H (2016) Research status and development trend of pantograph contact strip materials. Matec Web of Conf 67:06040
137. Shibata K, Yamaguchi T, Mishima J et al (2008) Friction and wear properties of copper/carbon/RB ceramics composite materials under dry condition. Tribol Online 3(4):222–227
138. Jiang X, Song T, Shao Z, Liu W, Zhu D, Zhu M (2017) Synergetic effect of graphene and MWCNTs on microstructure and mechanical properties of Cu/Ti3SiC2/C nanocomposites. Nanoscale Res Lett 12(1):607
139. Ngai TL, Lu L, Chen J, Zhang J, Li Y (2014) Preparation of SiC reinforced Ti3SiC2-base composite and its biocompatibility evaluation. Ceram Int 40(4):5343–5348
140. Yang D, Zhou Y, Yan X, Wang H, Zhou X (2020) Highly conductive wear resistant Cu/Ti3SiC2(TiC/SiC) co-continuous composites via vacuum infiltration process. J Adv Ceram 9:83–93
141. Aydin I, Karakose M, Akin E (2015) Anomaly detection using a modified kernel-based tracking in the pantograph-catenary system. Expert Syst Appl 42(2):938–948
142. Arnold M, Simeon B (2000) Pantograph and catenary dynamics: a benchmark problem and its numerical solution. Appl Numer Math 34(4):345–362
143. Liu Z (2017) Slide plate fault detection of pantograph based on image processing. In: Detection and Estimation Research of High-speed Railway Catenary. Advances in High-speed Rail Technology, Springer, Singapore, pp 109–137
144. Judek S, Jarzębowicz L (2013) 3D-scanning system for railway current collector contact strips. Comput Electr Eng 11:328–335
145. Li C, Ping L, Ma L (2010) A camera on-line recalibration framework using SIFT. Vis Comput 26(3):227–240
146. Dwarakanath D, Griwodz C, Halvorsen P, Lildballe J (2015) Online re-calibration for robust 3D measurement using single camera-pantolnspect train monitoring system. In: international conference on computer vision systems, Springer International Publishing, pp 498–510

147. Lee YJ, Lee JR, Ihn JB (2018) Composite repair patch evaluation using pulse-echo laser ultrasonic correlation mapping method. Compos Struct 204:395–401
148. Yu L, Tian Z (2016) Guided wave phased array beamforming and imaging in composite plates. Ultrasonics 68:43–53
149. Deng Q, Wei W, Yin G et al (2021) The effect of thermal shock temperature difference on the structural, dynamics and mechanical properties of carbon materials characterized by ultrasonic test technology. J Mater Sci 56(33):18522–18533
150. Aydin I (2015) A new approach based on firefly algorithm for vision-based railway overhead inspection system. Measurement 74:43–55
151. Ostlund S, Gustafsson A, Buhrkall L, Skoglund M (2008) Condition monitoring of pantograph contact strip. In: 4th IET international conference on railway condition monitoring. Derby, IET, pp 37–37
152. Wei W, Song Y, Yang Z, Wu G et al (2019) Investigation of the impacts of thermal shock on carbon composite materials. Mater (Basel) 12(3):435
153. Post W, Kersemans M, Solodov I et al (2017) Non-destructive monitoring of delamination healing of a CFRP composite with a thermoplastic ionomer interlayer. Compos Part A Appl Sci Manuf 101:243–253
154. Li H (2020) Research on fault detection algorithm of pantograph based on edge computing image processing. IEEE Access 8:84652–84659
155. Karakose E, Gencoglu M, Karakose M, Aydin I, Akin E (2016) A new experimental approach using image processing based tracking for an efficient fault diagnosis in pantograph-catenary systems. IEEE Trans Ind Inform 13(2):635–643
156. Na KM, Lee K, Shin SK, Kim H (2020) Detecting deformation on pantograph contact strip of railway vehicle on image processing and deep learning. Appl Sci 10(23):8509
157. Aydin I, Karakose M, Akin E (2014) A new contactless fault diagnosis approach for pantograph-catenary system using pattern recognition and image processing Methods. Adv Electr Comput En 14(3):79–88
158. MA L, Wang ZY, Gao XR et al. (2009) Edge detection on pantograph slide image. In: 2nd IEEE international congress on image and signal processing, Tianjin, pp 1–3
159. Kin E, Cheng W (2006) Pioneer design in automatic pantograph wear monitoring. Eng Struct 19(1):12–17
160. Hamey LGC, Watkins T, Yen SWT (2007) Pancam: In-service inspection of locomotive pantographs. In: 9th biennial conference of the Australian pattern recognition society on digital image computing techniques and applications (DICTA 2007). IEEE, Glenelg, pp 493–499
161. Landi A, Menconi L, Sani L (2006) Hough transform and thermo-vision for monitoring pantograph-catenary system. Proc Inst Mech Eng Part F J Rail Rapid Transit 220(4):435–447
162. Hu X, Chen Y, Yao X, Zhang Y et al. (2017) Research on abrasion detection technology of the pantograph slipper of urban rail train. In: Proceedings of the 3rd international conference on electrical and information technologies for rail transportation (EITRT). Springer, Singapore, pp 333–342
163. Aydin İ, Karaköse E, Karaköse M et al. (2013) A new computer vision approach for active pantograph control. In: 2013 IEEE INISTA, Albena, pp 1–5
164. Zhu X, Gao X, Wang Z, Wang L, Yang K (2010) Study on the edge detection and extraction algorithm in the pantograph slipper's abrasion. In: international conference on computational and information sciences, Chengdu, China. IEEE, pp 474–477
165. Crosby R (2008) Curvelet decomposition for detection of cylindrical targets. In: 15th IEEE international conference on image processing, San Diego, CA, USA. IEEE Press, Piscataway, pp 2832–2835
166. Kazemi FM, Izadian J, Moravejian R et al. (2008) Numeral recognition using curvelet transform. In: IEEE/ACS international conference on computer systems and applications, Doha, Qatar. IEEE Press, Piscataway, pp 606–612
167. Wu G, Gao G, Wei W et al (2019) Diagnosis and detection of service performance of pantograph and catenary. The electrical contact of the pantograph-catenary system. Springer, Singapore, pp 221–277